Wireless Personal Communications (2021) 121:3085–3123
https://doi.org/10.1007/s11277-021-08865-7

Check for updates

Performance Analysis of Parallel Concatenation of LDPC Coded SISO-GFDM System for Distinctive Pulse Shaping Filters using USRP 2901 Device and its Application to WiMAX

Nagarjuna Telagam[1,2] · **S. Lakshmi**[1] · **Nehru Kandasamy**[3]

Accepted: 8 August 2021 / Published online: 23 August 2021

Abstract

The increasing demand for high data rates requires channel error control codes for the upcoming fifth generation. This article presents an investigation of the parallel concatenation of low-density parity-check codes (PC-LDPC) in the fifth generation proposed waveform candidate called generalized frequency division multiplexing (GFDM). PC-LDPC codes are obtained by dividing the long and high complexity single LDPC codes into small two lower complexity codes, and these designed codes are applied to the 5G-GFDM waveform. Since the GFDM signal transmits data in both the time and frequency domain, these PC-LDPC codes can deal with two-dimensional errors. This channel coded GFDM system is integrated into Universal software radio peripheral (USRP) device for real-time implementation. The Attainment of the proposed transceiver is verified by computation of BER under distinctive channel coding techniques like convolutional, Golay, Bose-Chaudhuri-Hochquenghem (BCH), extended length single LDPC code. The different pulse shaping filters such as Raised Cosine (RC), Root Raised Cosine (RRC), Gaussian, and Xia 4th order filter are applied to the GFDM under the Gaussian noise and Rayleigh fading channel to compute Out of band (OOB) power. The PC-LDPC coded GFDM outperforms LDPC by 6.5 dB in the RRC filter for roll-off factor rate 0.5 under the Rayleigh fading channel. PC-LDPC code outperforms LDPC code with a coding gain of 2 dB was observed in IEEE 802.16 Transceiver.

Keywords GFDM · PC-LDPC · LDPC · USRP · RC · RRC · XIA · BER

✉ Nagarjuna Telagam
nagarjuna473@gmail.com

S. Lakshmi
slakmy@yahoo.co.in

Nehru Kandasamy
nnehruk@gmail.com

[1] Dept of Electronics and Communication Engineering, Sathyabama Institute of Science and Technology, Jeppiaar Nagar, Chennai 600119, India

[2] GITAM University, Bangalore, India

[3] Dept of Electrical and Computer Engineering, National University of Singapore, 21 Lower Kent Ridge Road, Singapore 119077, Singapore

1 Introduction

The GFDM system accomplishment the white spaces in the spectrum. The brunt of non-orthogonal subcarriers of GFDM can be controlled by the properties of transmitter and digital receiver filters. The transmission is block-based on FFT [1]. The data arrangement in GFDM is made in blocks where every block has different subcarriers, and every subcarrier has various sub symbols. The pulse shaping filters are applied to every symbol separately [2]. This pulse shaping reduces the out of band radiation of transmitted signals [3]. This GFDM scheme can fulfil the requirements of 5G. The synchronization technique that reduces the spectral emission is proposed [4]. In order to improve the system performance and capacity of the channel, channel coding is required for future wireless communications. LDPC codes are used in the early 1990s and 2000 and used in digital video broadcasting, satellite communications applications. This article uses the LDPC code of block length 10^7, approached the Shannon limit within 0.0045 dB [5]. The difference between hamming and LDPC codes are in the matrix size. The LDPC codes have a sparse matrix code with a few ones in the matrix. Whereas Hamming code has a length code of 2^{m}-1 columns. the LDPC codes parity check matrix depends on the transmitted data. The hamming code is related to cyclic coding theory [6, 7].

1.1 Associated Work

The forward error correction codes use redundancy bits to transmit the digital signal to detect and correct the received bits in the receiver side. The entire data block is employed to one code work in convolutional codes [8]. Other than convolutional codes, Golay codes, BCH codes, and RS codes [9] are also used as error correction and shows significant improvement in error-correcting capability [10]. The concatenation of codes is proposed in the channel encoder in the transmitter section. The convolutional codes are concatenated with reed Solomon codes to form turbo codes, which reaches performance near to Shannon limit. This turbo code uses iterative decoding algorithms in the receiver section. Another code proposed by Gallagher in 1961 is the low-density parity-check matrix; these codes show performance near the Shannon limit [11]. The turbo codes suffer from error floor in BER plots in high Signal-to-noise ratio areas because of low weight codeword [12]. The turbo receiver was designed in GFDM based cognitive radio to utilise feedback information for channel estimation [13]. The long block LDPC codes show better performance than turbo codes. However, the latency problem is identified in LDPC codes. In order to overcome that, concatenation of LDPC codes are proposed with the same iterative decoding algorithm, which is used in turbo codes as are the right choice for better performance [14]. The Dirichlet based pulse shaping filter reduces the OOB emission for the GFDM system; the BER analysis for guard symbols in the GFDM system was explained [15]. The novel proposed ramp filter is used as a pulse-shaping filter and reduces the OOB in GFDM corresponding to other filters [16]. The proposed pulse shaping filter has intense sharpness compare to RRC pulse in GFDM, and the Symbol error probability is calculated [17]. The SISO-GFDM transceiver was designed in a virtual and remote lab, and its characteristics are compared with the 4G-OFDM system [18]. A Quasi-cyclic LDPC decoder was designed using the NI USRP device and provides 2.4 Gb/s [19]. The audio signal transmission was tested in hard decoding in LDPC decoder for 32-bit codeword using USRP devices [20]. A

71% improvement in the complexity of receiver design was observed in computer-based simulation for LDPC code concatenated with staircase codes [21]. The parallel concatenation of LDPC codes with different compositions is elucidated in the survey article [22]. A significant reduction in BER was observed in 5G-GFDM when the concatenation of LDPC code with Turbo codes are used as channel coding schemes [23].

1.2 Scope of the Paper

The investigation of PC-LDPC codes with a 5G GFDM system over Gaussian noise and flat fading Rayleigh channel for distinctive prototype filters is analyzed in this paper. The BER performance is compared with other channel coding schemes. To identify the best pulse shaping filter, which provides less out of band power and efficient BER values in the GFDM system. To propose the novel GFDM transceiver design with high coding gain and less complexity decoder in receiver. They are furthermore exploring the PC-LDPC-GFDM transceiver by incorporating the WiMAX model for improvement in BER.

1.3 Organization of the Paper

This paper is categorized into Passage 1 accord the establishment about the GFDM, and its related work in the area of the field, the scope of the proposed system and organization of the article. Passage 2 explains the implementation and simulation parameters of LabVIEW based GFDM transceiver. Passage 3 explains the mathematical analysis of GFDM and parallel concatenation of LDPC codes using diagrams. Passage 4 discusses the USRP 2901 device, incorporation of PC-LDPC-GFDM system with IEEE 802.16 standard, and simulation parameters used by the user for GFDM transceiver. Passage 5 gives information about VI Programming for GFDM Using USRP Device, Sect. 6 and 7 explains the results achieved and Conclusions.

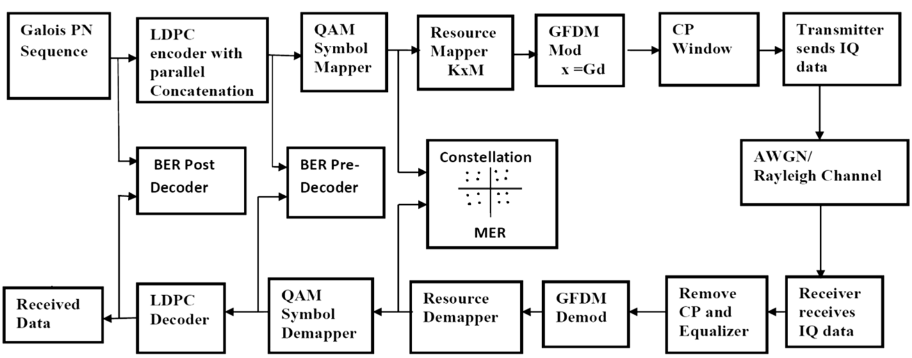

Fig. 1 General Block diagram of Proposed GFDM transceiver using USRP 2901

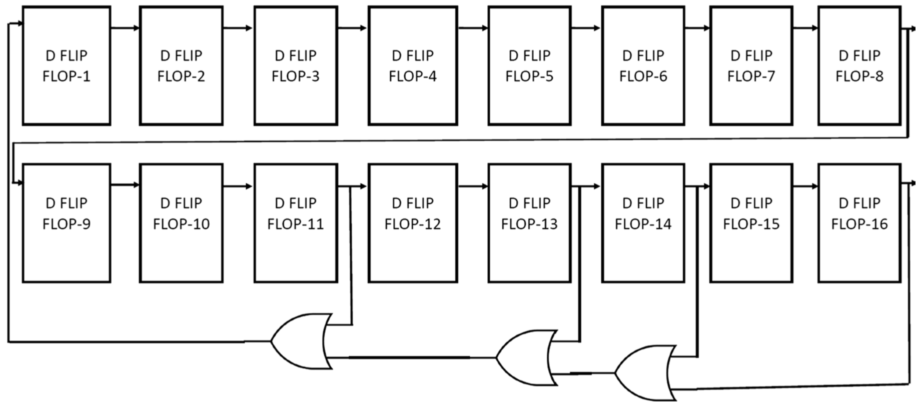

Fig. 2 Galois Linear Feedback shift register (LFSR) generation of PN Sequence

2 Channel Coded GFDM model

Figure 1 presents the block design of the GFDM system. The 16-bit PN sequence is used, which generates 65,535 bits. The generation of 16 bits can be done using a linear feedback shift register (LFSR), with tap positions at [1, 11, 13, 14, 16], as shown in Fig. 2. The PC-LDPC codes are formed by dividing the long length LDPC codes into two short block regular LDPC codes with H matrix as parity check matrix. The corresponding bits are

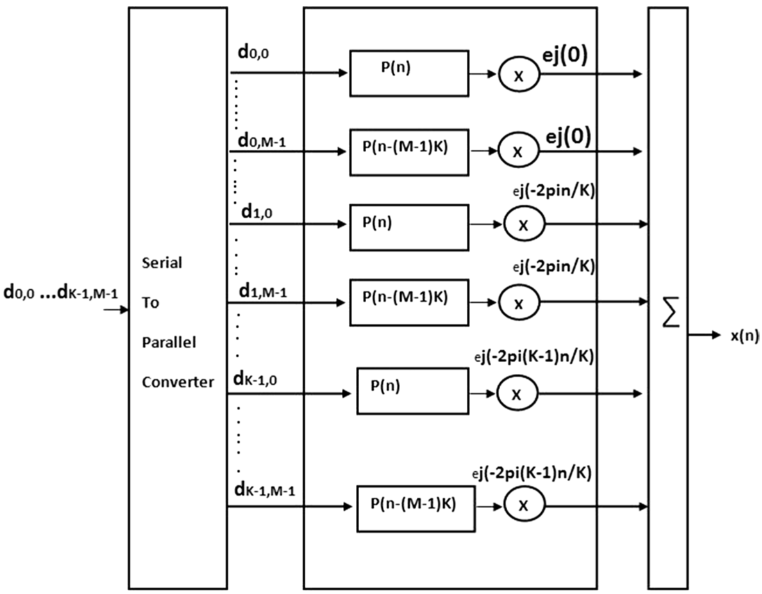

Fig. 3 GFDM modulator

converted to complex data symbols with QAM or BPSK modulation schemes. These complex data symbols are assigned to the resource mapper, which converts the data into the two-dimensional format using the GFDM modulation block structure, as shown in Fig. 3. One cyclic prefix is added for the entire GFDM block, whereas in OFDM, one cyclic prefix is added for each symbol. Since the USRP device is used, it converts the transmitted bits into IQ samples data. the verto antenna transfers the data into free space. The received data is a combination of AWGN channel or Rayleigh fading channel along with environmental noise. These data are processed through the FPGA receiver, and these IQ data samples are transferred through the GFDM receiver section. In the receiver section, removing of cyclic prefix symbol, if zero padding is included in the transmitter, the zero-padding is also removed in the receiver. The channel estimation is used to predict the estimation of the received symbol. The decoding of the PC-LDPC codes are also done with the help of two single LDPC decodes followed by deinterleaver.VI. Once the PC-LDPC decoder reaches the maximum number of iterations, the decoder stops performing, and the output is recei ved.

The VI hierarchy of the GFDM LabVIEW program is viewed in Fig. 4.

Figure 4 shows the list of Virtual instrumentation programs used in the proposed design. The sequence of steps followed by the transmitter, receiver its sub-VI's are mentioned in the above Figure. The sequence of Virtual instrumentation programming is explained.

3 List of VI's in GFDM Transmitter

3.1 Galois Pseudo Random Noise Generator VI (Message Source)

The Galois PN sequence generation is shown in Fig. 2. With the help of LFSR, D flip flop has m input bits, the length of the PN sequence is $N = 2^{m} - 1$. The tap positions are [1, 11, 13, 14, 16], the 16-bit input is used. Equation (1) is shown mathematical form of message bits generation.

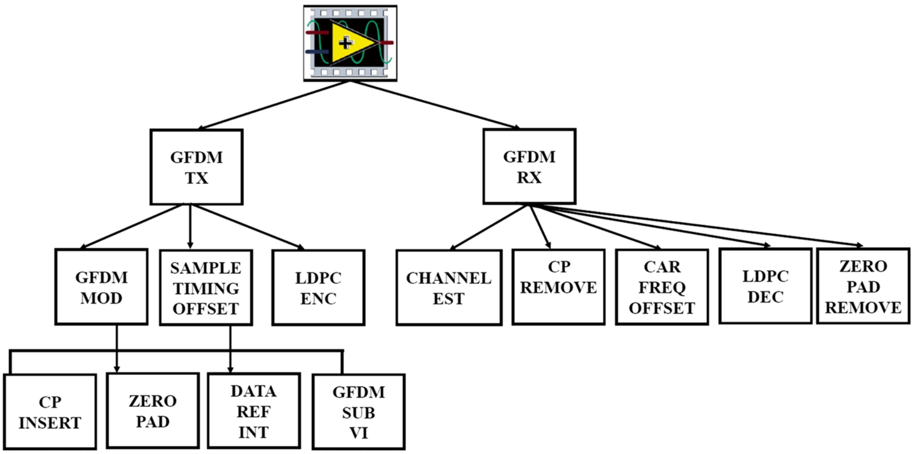

Fig. 4 Virtual Instrumentation Hierarchy

$$M^{(16)}(x) = 1 + x^{1} + x^{13} + x^{14} + x^{16} \tag{1}$$

3.2 Symbol Mapper and Prototype Filter VI's

The source encoder instance VI maps the input bits to complex symbols. The modulation scheme used here is QAM and BPSK schemes. With 2^{Δ} Constellation size Δ is the order of the modulation. The symbol map is an array which maps every symbol in the complex baseband modulated waveform. The VI calculates the impulse response of the filter using Eqs. (2) and (3). Mainly four pulse shaping filters are chosen for GFDM system design. These prototype filters and their impulse response are shown in Eqs. (2), and (3), (4), and (8). The filters are RC, RRC, Gaussian pulse, and Xia 4th order filter. The Eqs. (5), (6) and (7) are the functions of Xia 4th order filter. In every impulse response of the filter, α is the roll-off factor. For every pulse shaping filter, the roll-off factor plays an essential role in controlling the signals out of the band emission spectrum. It helps in reducing the latency of the system. However, we observed that the BER of the system also depends on roll-off factor values. Hence, we identified two unique values of roll factor values to compute BER and plot the response.

$$P_{RC}(t) = \sin c\left(\frac{t}{T}\right)\frac{\cos(2\Pi\alpha t)}{1-(\frac{2\alpha t}{T})^2} \tag{2}$$

$$P_{RRC}(t) = \frac{\sin\left(\frac{\Pi t}{T(1-\alpha)}\right) + \frac{4\alpha t}{T\cos\left[\frac{\Pi t}{T}(1+\alpha)\right]}}{\Pi t/T\left[1-\left(4\alpha t/T\right)^2\right]} \tag{3}$$

$$P_{gaussian}(t) = \frac{\sqrt{\pi}}{\alpha}e^{\left(\frac{-\pi^2 t}{\alpha^2 N}\right)} \tag{4}$$

$$Xia(t) = 1, \quad if\,|t| \le \frac{(1-\alpha)KT_s}{2} \tag{5}$$

$$Xia(t) = \frac{1}{2}(1 + e^{j\pi P_{Xia}}(t), \quad if\,\frac{(1-\alpha)KT_s}{2} < |t| \le \frac{(1+\alpha)KT_s}{2} \tag{6}$$

$$Xia(t) = 0, \quad if\,\frac{(1+\alpha)KT_s}{2} < |t| \tag{7}$$

$$P_{Xia}(t) = \left(\frac{|t| - \left(\frac{(1-\alpha)KT_s}{2}\right)}{\alpha T}\right) \tag{8}$$

These four prototype filters p [.] can be used for GFDM, which has a maximum impact on Out of band (OOB) power and BER plot response.

3.3 Mathematical Model of GFDM Modulator

The different operations are performed on the $d_{k,m}$ (data vector). The serial to parallel converter converts this data vector into parallel data streams. The mapped data is divided into K subcarriers having M subsymbols, i.e., shown in Eq. (9). The mathematical modelling of GFDM was carrying out in the article [4].

$$\overrightarrow{d_{k,m}} = (d_{0,m}, \ldots\ldots d_{K-1,m})^T \tag{9}$$

After converting the serial data to parallel, the pulse shaping operation is performed on each data symbol separately, as represented by Eq. (10).

$$P_{k,m}[n] = P[(n - mk) \bmod N]e^{-j2\pi \frac{kn}{k}} \tag{10}$$

The transmit samples x(n), as shown in Eq. (11), is attained by superpositioning the transmitted symbols, n = 0, 1,……..N-1

$$x(n) = \sum_{k=0}^{K-1} \cdot \sum_{m=0}^{M-1} \cdot p_{k,m}[n] * d_{k,m} \tag{11}$$

$$y(n) = GF \cdot \overrightarrow{x(n)} + \overrightarrow{w(n)} \tag{12}$$

in which GF is a channel matrix

$$GF = \left(NS + Ns_{cp} + Ns_{ch} - 1\right)x\left(Ns + Ns_{cp}\right), where\, Ns = KM \tag{13}$$

Ns is the number of symbols, which is equal to the multiplication of subcarriers and sub symbols. After modulation of the transmitted signal, the cyclic prefix is added at the end of the GFDM block with length K/4.

$$y_{cp}(n) = x_{cp}(n) + w(n) \tag{14}$$

Due to the Intersymbolic interference problem in the channel, the zero-forcing equalizer is performed to get the desired signal.

$$ZF = GF^{-1}GFx(n) + GF^{-1}w(n) \tag{15}$$

$$ZF = x(n) + w(n) \tag{16}$$

$$GF_{ZF} = (GF^H GF)^{-1} GF^H \tag{17}$$

$$d_r = GF_{ZF} \cdot Z \tag{18}$$

The desired signal can be obtained from the noisy channel using zero forcing equalizer is explained mathematically using equations from (14), (15), (16), (17) and (18).

3.4 Encoding Sequence of Parallel Concatenation of LDPC codes (PC-LDPC)

the encoding process of PC-LDPC codes is explained with the parity check matrix H matrix of size 6 × 12. The number of ones is always greater than several zeros in the matrix. The code rate R is R = [(N-M)/N], N = 12 and M = 6, which are several columns and rows in the matrix. The Tanner graph, which helps in the decoding of LDPC, is shown in Fig. 5. The variable nodes and parity nodes are of lengths 12 and 6 as shown in Eq. (19). The variable nodes and parity nodes are represented by $N_m[m\varepsilon\{1....N\}$ and $M_n(n\varepsilon\{1....M\})$

$$H = \begin{bmatrix} 1&1&0&0&1&1&0&1&0&0&0&1 \\ 1&1&1&0&0&1&1&0&1&0&0&0 \\ 0&0&0&1&1&0&0&1&1&1&0&1 \\ 0&0&1&1&0&1&0&0&1&1&1&0 \\ 1&0&1&0&0&0&1&0&0&1&1&1 \\ 0&1&0&1&1&0&1&1&0&0&1&0 \end{bmatrix} \tag{19}$$

The PC-LDPC codes are formed by using the same length regular LDPC encoders with R = ½ and MT Permute Interleaver.VI is used in between the two LDPC encoders. With the help of an old technique called the LU decomposition method, the decoding process of concatenation is explained below. The H network into two sections, i.e., H_1 and H_2 as shown in Eq. (20). Each partitioned H grid is again utilized in the LU decay framework. i.e., to discover the lower triangular network and upper triangular lattice. i.e., the lower triangular lattice comprises each of the zeros over the corner-to-corner components. Thus, the upper triangular network comprises each of the zeros underneath the diagonal components.

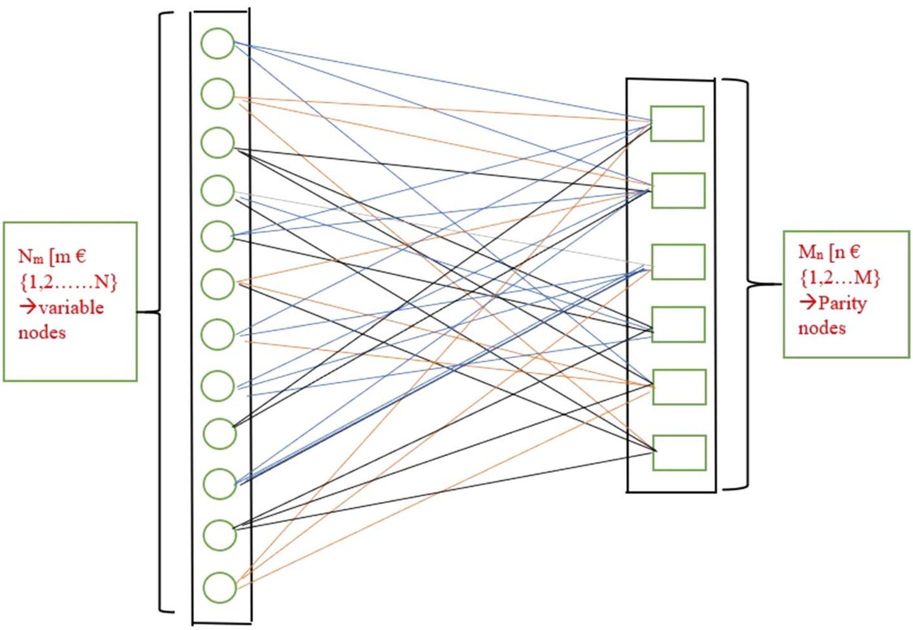

Fig. 5 LDPC Constraint graph (Tanner)

$$H = [H_1][H_2] \tag{20}$$

$H_1 = [H_{L1}\ H_{U1}]$, $H_2 = [H_{L2}\ H_{U2}]$, LXU = H, UXL # H,
The factorization of H_1 MXM.

$$H_{L1} = \begin{bmatrix} 1 & 0 & 0 & 0 & 0 & 0 \\ 1 & 1 & 0 & 0 & 0 & 0 \\ 0 & 0 & 1 & 0 & 0 & 0 \\ 0 & 0 & 0 & 1 & 0 & 0 \\ 1 & 1 & 0 & 0 & 1 & 0 \\ 0 & -1 & 1 & 0 & 0 & 1 \end{bmatrix} H_{U1} = \begin{bmatrix} 1 & 1 & 0 & 0 & 1 & 1 \\ 0 & -1 & 1 & 0 & -1 & -1 \\ 0 & 0 & 1 & 1 & 0 & 1 \\ 0 & 0 & 0 & 1 & 1 & 0 \\ 0 & 0 & 0 & 0 & 0 & -1 \\ 0 & 0 & 0 & 0 & 0 & -2 \end{bmatrix}$$

The factorization of H_2 MX(N−M).

$$H_{L2} = \begin{bmatrix} 1 & 0 & 0 & 0 & 0 & 0 \\ 0 & 1 & 0 & 0 & 0 & 0 \\ 0 & 1 & 1 & 0 & 0 & 0 \\ 1 & 0 & -1 & 1 & 0 & 0 \\ 0 & 0 & 1 & 0 & 1 & 0 \\ 1 & 1 & -1 & 0.5 & 0.5 & 1 \end{bmatrix} H_{U2} = \begin{bmatrix} 1 & 0 & 1 & 0 & 0 & 0 \\ 0 & 1 & 0 & 0 & 0 & 1 \\ 0 & 0 & 1 & 1 & 0 & 0 \\ 0 & 0 & 0 & 2 & 1 & 1 \\ 0 & 0 & 0 & 0 & 1 & 0 \\ 0 & 0 & 0 & 0 & 0 & -1.5 \end{bmatrix}$$

The codeword C_W is the concatenation of information block C_{IB} and redundancy block C_{RB} is shown in Eq. (21).

$$C_w = [\, C_{RB}\ \ C_{IB} \,] \tag{21}$$

From the properties of the H matrix, substitute Eq. (21) and Eq. (20) in Eq. (22). C_W = codeword, information block C_{IB}, redundancy block C_{RB}, parity check matrix is H, $H_{L1,}$ H_{L2} is the lower triangular matrixes, $H_{U1,}$ H_{U2} is the upper triangular matrixes. Transpose of H matrix multiplied by codeword is equal to zero. The redundancy bits allow the user to add extra bits to the information bits for ensuring no data is lost in the total block of data. this redundancy bits also helps the receiver to detect or correct the errors. To avoid the computational complexity, the parity check matrix is divided into LU matrix as shown in below equations.

$$C_W H^T = 0 \tag{22}$$

$$C_{RB} H_1^T + C_{IB} H_1^T = 0$$

$$C_{RB} \left[H_{L1}^T . H_{U1}^T \right] + C_{IB} H_{U1}^T = 0$$

$$C_{RB} H_{L1}^T \cdot H_{U1}^T = C_{IB} H_{U1}^T$$

$$H_{L1}^T \left(C_{RB} \cdot H_{U1}^T \right) = C_{IB} H_{U1}^T$$

$$let Y = C_{RB} \cdot H_{U1}^T \; and\, Z = C_{IB} H_{U1}^T$$

$$H_{L1}^T Y = Z, Y = \frac{Z}{H_{L1}^T}$$

$$C_{RB} = \frac{Y}{H_{U1}^{T}} \tag{23}$$

The redundancy block can be obtained by using above Eq. (23).

The first component, encoder1 encodes the information block.

$$C_{RB}^{1}C_{IB}^{1} = [C_{RB1}^{1}C_{RB2}^{1}.....C_{RBM}^{1}C_{I}^{1}C_{2}^{1}.....C_{N-M}^{1}] \tag{24}$$

$C^{1}{}_{RB}$ is the parity matrix block of the first encoder output. The output of the first encoder is applied to interleaver.VI to generate the $C^{1}{}_{I}$.interleaved data of the systematic block. The encoder2 uses only the interleaved output data. The output of the interleaved circuit is given as $C^{2}{}_{IB} = C_{IB}$ interleaved is applied to the second encoder. Figure 6 shows the encoding process.

$$[C_{RB}^{2}C_{IB}^{2}] = [C_{RB1}^{2}C_{RB2}^{2} \dots ..C_{RBM}^{2}C_{1}^{2}C_{2}^{2} \dots \dots C_{N-M}^{2}] \tag{25}$$

The second encodes the information block C_I

$$C_I = [C_1C_2......C_{N-M}] \tag{26}$$

$$[C_{RB}^{1}C_{RB}^{2}C_{I}^{2}] = [C_{RB1}^{1}C_{RB2}^{2}......C_{RBM}^{1}C_{RB1}^{2}C_{RB2}^{2}....C_{RBM}^{2}C_{1}^{2}C_{2}^{2}.. \dots C_{N-M}^{2}] \tag{27}$$

Equation (27) is concatenation of information block, redundancy parity blocks.

3.5 PC-LDPC Decoding Process

Soft in soft out (SISO) message-passing decoding algorithm is used for decoding single LDPC code.

Each Part of the code is decoded by the soft in the soft out (SISO) algorithm. The decoder receives the soft outputs $C^{2}{}_{RB}$,$C^{1}{}_{RB}$, $C^{2}{}_{IB}$. In which $C^{2}{}_{IB}$, $C^{1}{}_{RB}$ and $C^{2}{}_{RB}$ Represents the received block corresponding to the interleaved block and received blocks and parity blocks of second and first decoders are shown in Eq. (28). The first iteration generates the soft information blockI^2, i.e., the LDPC decoder2 results $inI^2 = [I^{2}{}_{1}I^{2}{}_{2}.....I^{2}{}_{N-M}]$ with the input Eq. (29) as shown in Fig. 7.

$$[C_{RB}^{2}C_{IB}^{2}] = [C_{RB1}^{2}C_{RB2}^{2} \dots ..C_{RBM}^{2}C_{1}^{2}C_{2}^{2} \dots .C_{N-M}^{2}] \tag{28}$$

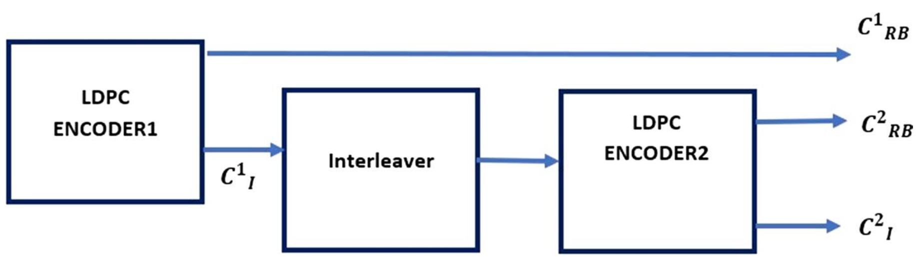

Fig. 6 The parallel concatenation of LDPC using two regular LDPC codes with R = ½

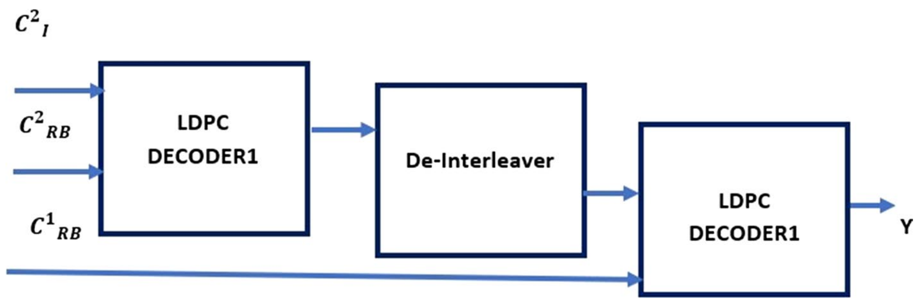

Fig. 7 Decoding process of PC-LDPC using SISO

The LDPC decoder1 results in the soft information I^1 using the received block $C^1{}_{RB}$ and the soft information I^2 generated by first LDPC decoder 2; the resultant equation is shown as (30)

$$\left[C^1_{RB} I_d\right] = \left[C^1_{RB1} C^1_{RB2} \ldots C^1_{RBM} I^1_d I^2_d \ldots . I_{dN-M}\right] \tag{29}$$

Considering the next iteration, the first LDPC decoder2 uses the soft information I^1 generated by the second LDPC decoder1 to do the decoding process, the input for the decoder is shown in Eq. (31)

$$\left[Y^2 I\right] = \left[Y^2_1 Y^2_2 \ldots . Y^2_M I_1 I_2 \ldots I_{N-M}\right] \tag{30}$$

$$I = x^2 + I_{INTERLEAVER} \tag{31}$$

The interleaver and deinterleaver blocks in the output of LDPC decoder1 and decoder 2 are used to decorrelate the soft decision at the output of each decoder. After the maximum number of iterations (MaxIT) reach the decoder stops working, and LDPC decoder1 generates the output Y. the output along with concatenation of soft information I are shown in Eq. (30). The sequence of decoding steps followed in this design is the SUM-PRODUCT algorithm [24].

3.6 AWGN and Rayleigh Channel VI

The two channels are employed to GFDM complex waveform, and the two channels are time-varying channels. The first channel is Gaussian noise, and the second channel is Rayleigh fading channel. These channel VI's are already inbuilt in the LabVIEW programming models; the environmental noise is also added to the GFDM waveform along with two channels. The AWGN VI is utilized in which the user can determine E_b/N_0. The qualities of the channel can be varied with channel frequencies from 100 to 900 Hz. Figure 8 shows MT add AWGN.VI with IQ impairments. The data type of signal is pink color, a complex IQ GFDM signal applied to MT Apply IQ impairments.VI program.

The GFDM complex signal is applied to selective fading.VI, the fading profile is selected, such as flat fading or fast fading or slow fading, frequency selective fading. The MT generates a fading profile.VI is applied to the selective fading profile.VI block. The selective Rayleigh fading (jakes model) has been selected for this transceiver. The Jake

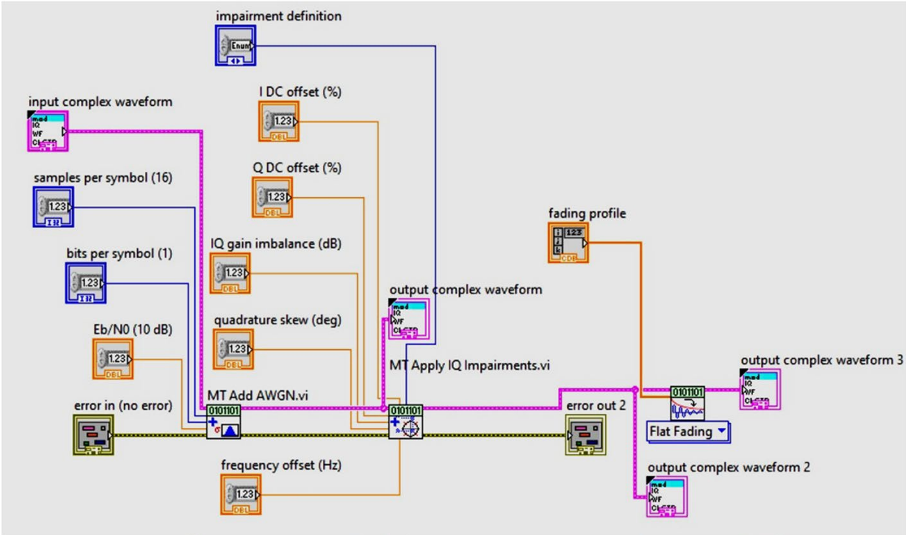

Fig. 8 MT add AWGN.VI and MT Apply IQ Impairments.VI

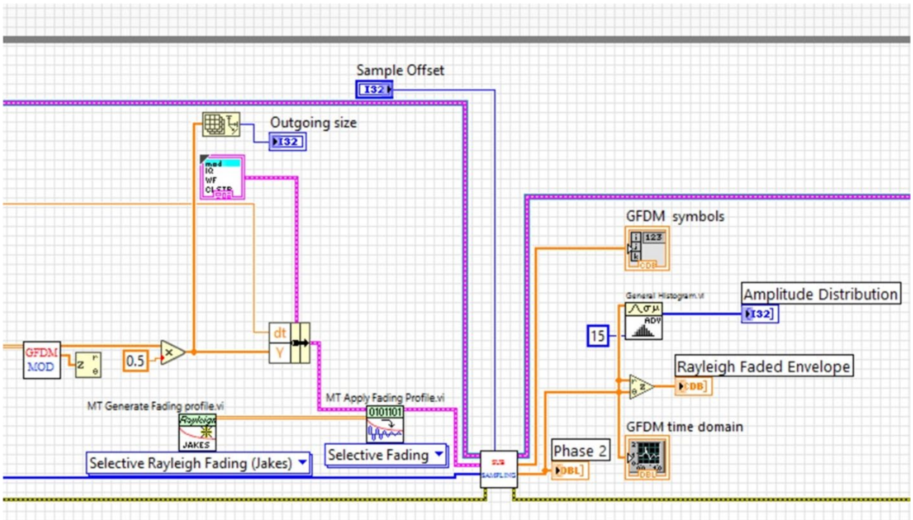

Fig. 9 MT fading profile.VI (Rayleigh Fading channel) and Apply fading profile.VI

model consists of frequency oscillators, and they generate sinusoidal oscillations based on components present in the feedback circuit as shown in Fig. 9.

4 USRP 2901 Radio Transceiver Working Sequence for PC-LDPC Codes with GFDM

This section explains the two USRP 2901 devices used, which transmits the IQ data from the verto antenna and receives the combination of IQ data with AWGN channel noise along with environmental noise. This USRP radio transceiver is tested for different channel coding techniques for determining the performance analysis of the GFDM system under the AWGN channel. The exact process is again repeated for the Rayleigh fading channel.

5 Transceiver Blocks in USRP Device

The user PC propagates the IQ signals and send them to a radio device through the universal serial cable. The upconverter changes the IQ signals into 64 Mega samples per sec by using a mixer circuit. The BPF is used to pass the bandlimited signal to the frequencies of the USRP device ranging from 75 kHz to 2 GHz. The user can use any frequency for his application design. The verto antennas transmit the IQ samples to the free space environment. The receiver captures the IQ samples mixed with free space noise and sends them to receiver blocks. The Low noise amplifier amplifies the signal,

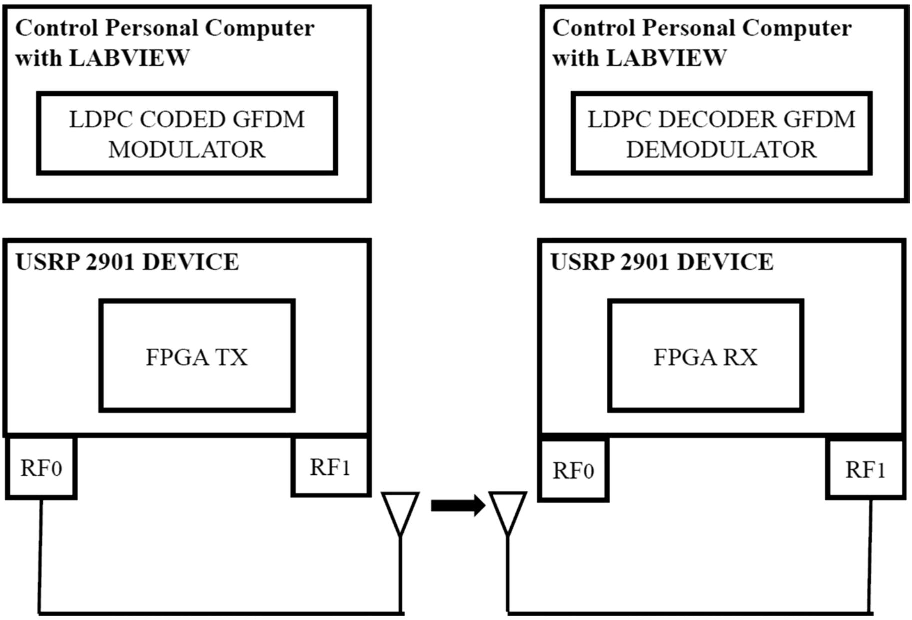

Fig. 10 Hardware setup of two USRP devices with GFDM modulator and demodulator

mixer down-converts the IQ samples and Analog to digital converter to convert the signal into user-specified rate [25]. Figure 10 is the schematic diagram of the hardware setup.

5.1 PC-LDPC/LDPC Codes based GFDM/OFDM-WIMAX System Design and Specifications

This system model is based on a 5G candidate waveform called GFDM, but the IEEE standard 802.16e supports only the OFDM model. Hence we proposed to convert the GFDM system into the OFDM model and then apply PC-LDPC codes are forward error-correcting codes before the interleaving section in the scenario. To convert the GFDM system into the OFDM model, the number of subsymbols should be equal to 1. i.e.(M = 1), then K increases to N, Number of subcarriers(K) goes to symbols(N), (without altering bandwidth), then the sufficient spacing between the subcarriers is present, then GFDM is converted to OFDM.

The term WiMAX is termed as Worldwide Interoperability for Microwave Access. It is formed in 2001 to increase the interoperability of wireless MAN, also called the IEEE 802.16 standard. WiMAX is an alternative to digital subscriber lines and cable. Wireless fidelity (Wi-Fi) uses carrier sense multiple access collision avoidance schemes in the MAC layer. But in WiMAX, the MAC layer uses a scheduling algorithm, which helps overcome the drawbacks of Wi-Fi. WiMAX operates in the frequency range of 2–11 GHz. OFDM technique is used to implement a WiMAX technique that overcomes all the drawbacks of the existing system. In this scenario, the parallel concatenation of LDPC codes are used as FEC codes; the MT permute interleaver.VI is used as interleaver, as shown in Fig. 11. The performance of this system is compared with single long length high complexity LDPC codes. The simulation parameters used to generate results are taken from Table 1.

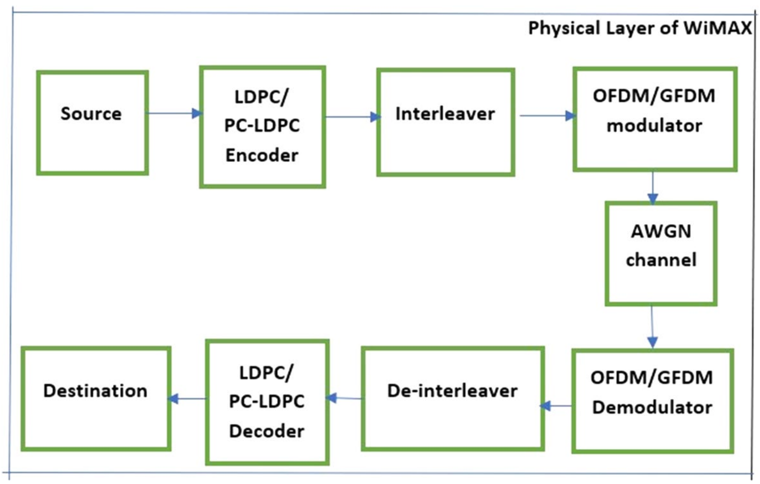

Fig. 11 PC-LDPC/LDPC as forward Error Correcting code in physical layer model of WiMAX

Table 1 Simulation parameters used in WiMAX model using PC-LDPC codes

S.No	Simulation parameters for WiMAX	Values
1	Modulation and Constellation size	BPSK/4-QAM
2	Carrier frequency	5.9GHZ
3	LDPC encoder and decoder/PC-LDPC encoder and decoder	Parity matrix is same as design in GFDM system
4	Code rate	½
5	2 step permutation interleaver process in transmitter and receiver	–
6	FFT size and no of subcarriers	128, 512
7	No of Subsymbols	1
8	Roll off factor value, RC Filter	0.23
9	Cyclic prefix and pilot symbol size	FFT/4 = 32 and 16

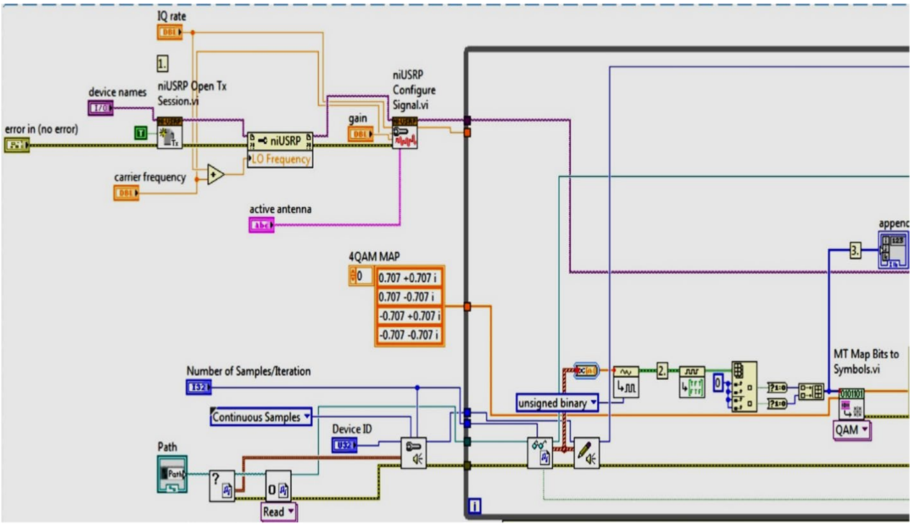

Fig. 12 Opening a USRP 2901 transmitter session

5.1.1 VI Programming for GFDM System using USRP Device

Figure 12 shows the USRP 2901 device starts transmission session; the VI required are niUSRP open Tx session.VI opens the session, followed by the configuration of the signal. VI, the IQ rate, carrier frequency, device names, a gain of the antenna in decibels, and active antennas numbers are user-defined.

Figure 13 shows the sequence of steps followed in the receiver section, the Ni USRP open Rx session.VI is used to open the receiver session, Ni USRP Fetch RX Data.VI Fetches complex, double-precision floating-point data in a waveform data type from the specified channel.

Figure 14 shows the GFDM system design with the parameters such as IQ gain imbalance, quadrature skew, roll-off factor value and a frequency offset value. This VI

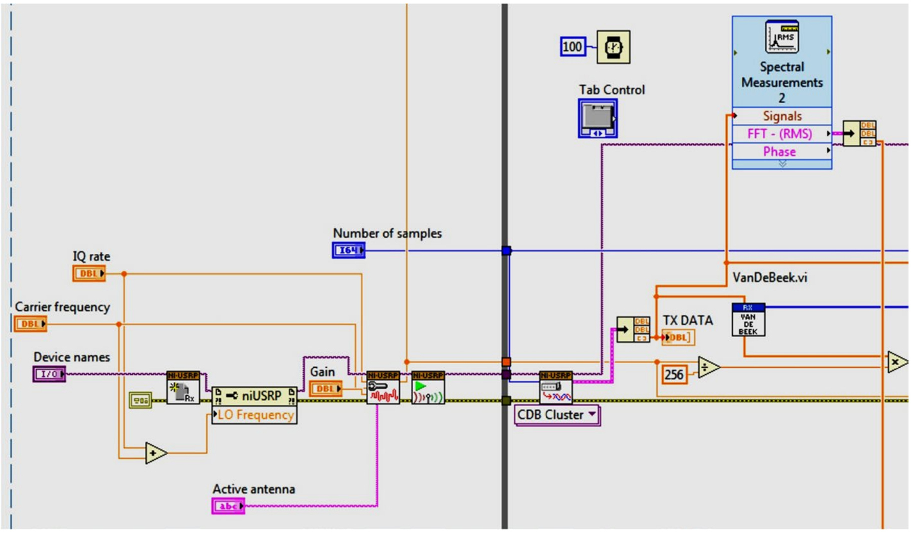

Fig. 13 Opening a USRP 2901 receiver session

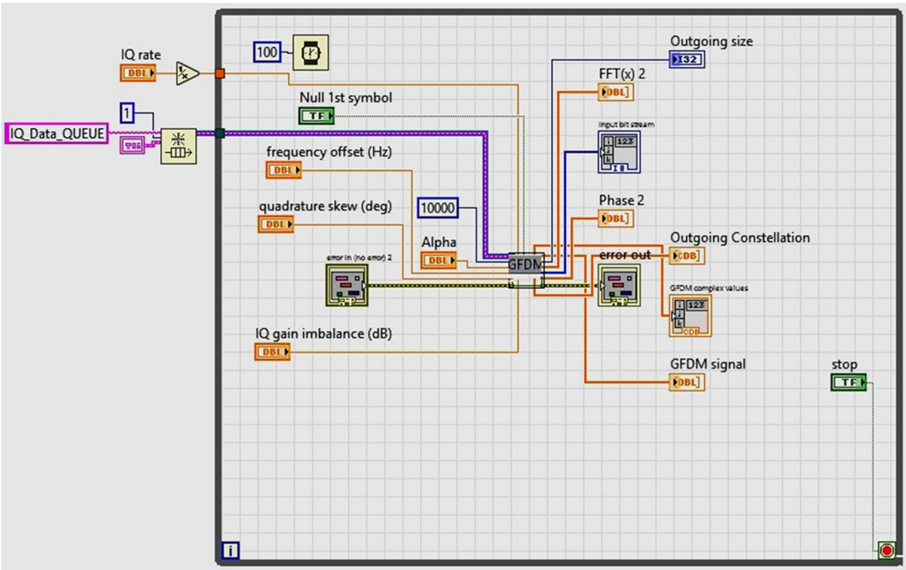

Fig. 14 GFDM system model design using LabVIEW programming

programming generates results for Tables 2 and 3, where the BER values are generated without employing channel coding schemes.

Figure 14 is the transmitter section for the WiMAX model. The number of subsymbols is equal to one, making the GFDM system model converted to the OFDM model. The simulation parameters used are shown in Table 1. Figure 15 shows the receiver model for the WiMAX model. Here, the LabVIEW programming based VI is used to generate the

Table 2 BER computation for E_b/N_0 at 5 dB for prototype filter in GFDM with roll-off factor values

"α" value	Raised Cosine prototype	Root Raised Cosine prototype	Guassian pulse filter	Xia filter of 4th order
	Bit Error Rate Computation under AWGN channel at E_b/N_0 value of 5 dB			
0.1	1.32xE-2	2.306xE-2	1.34xE-1	1.12xE-3
0.2	1.10xE-2	1.600xE-2	1.33xE-1	1.01xE-3
0.3	1.421xE-2	2.381xE-2	1.71xE-1	1.21xE-3
0.4	1.290xE-2	2.353xE-2	1.65xE-1	1.30xE-3
0.5	1.175xE-2	1.743xE-2	1.57xE-1	1.05xE-3
0.6	1.432xE-2	1.913xE-2	1.73xE-1	1.32xE-3
0.7	1.467xE-2	2.343xE-2	1.74xE-1	1.77xE-3
0.8	1.781xE-2	2.786xE-2	1.784xE-1	1.88xE-3
0.9	1.893xE-2	2.854E-2	1.893xE-1	1.97xE-3

Table 3 BER computation for E_b/N_0 at 20 dB for prototype filter in GFDM with roll-off factor values

"α" value	Raised Cosine prototype	Root Raised Cosine prototype	Guassian pulse shaping filter	Xia filter of 4th order
	Bit Error Rate Computation under AWGN channel at E_b/N_0 value of 20 dB			
0.1	3.12xE-4	3.10xE-4	3.34xE-2	2.02xE-5
0.2	3.00xE-4	3.00xE-4	3.33xE-3	2.01xE-5
0.3	3.52xE-4	3.48xE-4	3.71xE-3	2.41xE-5
0.4	3.69xE-4	3.55xE-4	3.65xE-3	2.80xE-5
0.5	3.105xE-4	3.84xE-4	3.57xE-3	2.15xE-5
0.6	3.732xE-4	3.91xE-4	3.73xE-3	2.52xE-5
0.7	3.867xE-4	3.94xE-4	3.74xE-3	2.87xE-5
0.8	4.181xE-4	3.98xE-4	3.784xE-3	2.98xE-5
0.9	4.293xE-4	4.254xE-4	3.893xE-3	2.99xE-5

received signal and compute the BER value. The list of VI's is used are CP removal.VI, which works to remove the cyclic prefix, CFO correction.VI works to correct the carrier frequency offset rate, BER.VI calculates the average BER for a given Galois PN sequence.

As clarified in the GFDM and VI Hierarchy system model in Fig. 4, the prototype filters such as RC, RRC, Gaussian, and Xia are chosen, the list of VI's utilized in the channel coded GFDM handset is shown in Fig. 16. The PC-LDPC encoders with block interleaver are connected to the GFDM modulator. PC-LDPC is constructed by breaking a long and high complexity of conventional single LDPC code into two smaller and lower LDPC codes. The regular parity check matrix is used as input for LDPC code and has three inputs n, j and k. where each variable represents iterations size, rows, and columns size. The generated GFDM symbol is again added to the AWGN/ Rayleigh fading channel. Table 4 shows all the simulation parameters used in GFDM.

The receiver of GFDM virtual programming as shown in Fig. 17 consists of PC-LDPC decoder, deinterleaver, the receiver blocks are already briefed in passage 2 and the list of VI hierarchy used. The primary algorithm used here is MIN SUM, the message passing with soft input and soft output iterations are explained in the passage 3.4 and 3.5. the same

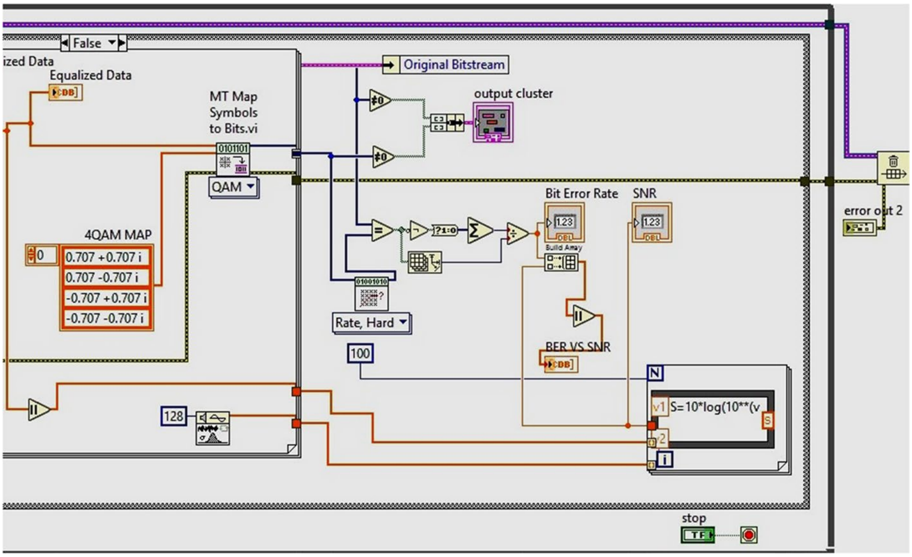

Fig. 15 GFDM/OFDM receiver model for WiMAX simulation parameters

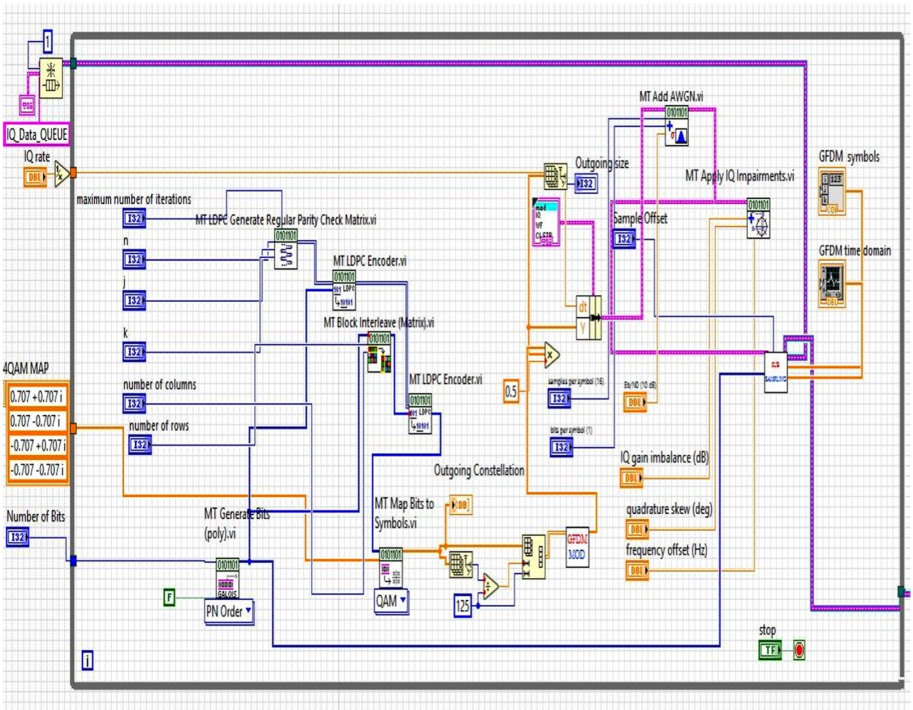

Fig. 16 VI for Proposed Transceiver for PC-LDPC coded GFDM system

Table 4 Transceiver simulation table

Serial No	Reconfigurable specifications of User	Values used by user
1	Galois's sequence	15,19
2	Eb/No	30 dB (or) any value
3	'α' roll-off factor	0.2, 0.5
4	Subsymbols M	1,15
5	Subcarriers K	128
6	No od symbols N = K*M	1920
7	Cyclic prefix(in µs) [Number of cyclic prefix multiple of subsymbol] Ncp = r*M, r = 1	15
8	Transmitter and receiver carrier frequency used in USRP 2901 device	910 MHz and 2 GHz
9	Transmitter and Receiver gain used in USRP 2901 device	3 dB, 6 dB
10	Digital Inphase and Quadrature components (IQ) values generated by USRP device	5 M samples/sec
11	No of bits used for QAM symbols/ BPSK	4,6
12	Transmitter session.VI, Receiver session.VI	Open a transmission session and receiver session for USRP device
13	VERT2450 antenna frequency range used in the USRP 2901 device	2.4 GHz
14	Radiation pattern and type of polarization used in VERT2450	Omnidirectional and Vertical

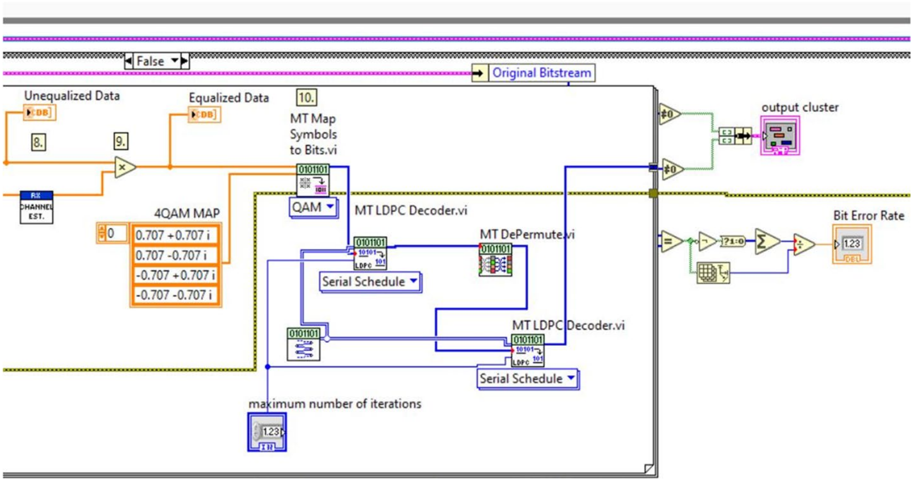

Fig. 17 GFDM Receiver VI

regular two LDPC decoders are used with deinterleaver present between them. The maximum iterations for the decoder are set as 30, 100, and 200. For different pulse shaping filters RC, RRC, and Xia 4^{th} order filter with different roll-off factor values, corresponding BER is calculated, the expressions are explained in Sect. 6. The mathematical equation of the Symbol error probability (SEP) performance of GFDM having 16-QAM data transmission in AWGN channel and Rayleigh fading channel is given in Eqs. (32), (33) and (34).

$$SEP = 2\left(\frac{K-1}{K}\right)erfc\left(\sqrt{a}\right) - \left(\frac{K-1}{K}\right)erfc^2\left(\sqrt{a}\right) \tag{32}$$

$$\Upsilon = \frac{3\frac{NS}{NS+N_{cp}+N_{cs}}}{2\left(2^{\nabla}-1\right)}\frac{E_s}{\varphi N_0} \tag{33}$$

$$SEP_{.} = \frac{2}{\left(\left(\frac{K-1}{K}\right)\left(1-\sqrt{\frac{\Upsilon}{1+\Upsilon}}\right)-\left(\frac{K-1}{K}\right)^2\left[1-\frac{4}{\pi}\sqrt{\frac{\Upsilon}{1+\Upsilon}}a\tan\left(\sqrt{\frac{1+\Upsilon}{\Upsilon}}\right)\right]\right)} \tag{34}$$

6 Result Analysis

Figure 18 shows the front panel output screenshot, in which k, j are rows and columns in the LDPC decoder. The maximum iterations of the decoder can be changed with the help of indicators, and the rayleigh envelope is plotted; the QAM constellation is plotted using the XY graph. The specifications of LDPC codes are n,j,k, MaxIT. n gives no of columns used, j gives no of ones in the column, j is always an odd number, k gives no of ones in a row, MaxIT specifies maximum no of iterations in a matrix that is not rank efficient, the PC-LDPC decoder will stops operation when the number of iterations exceeds the MaxIT.

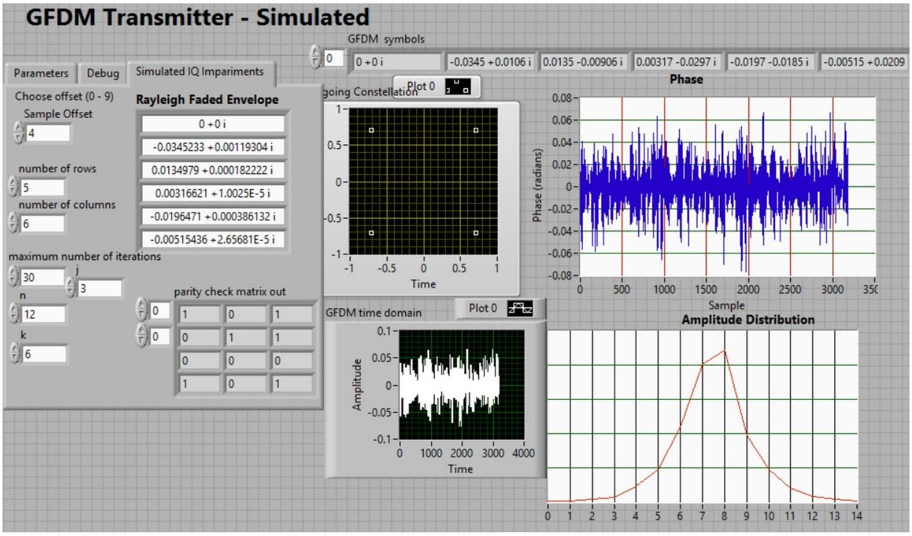

Fig. 18 GFDM-PC-LDPC decoder Receiver front panel

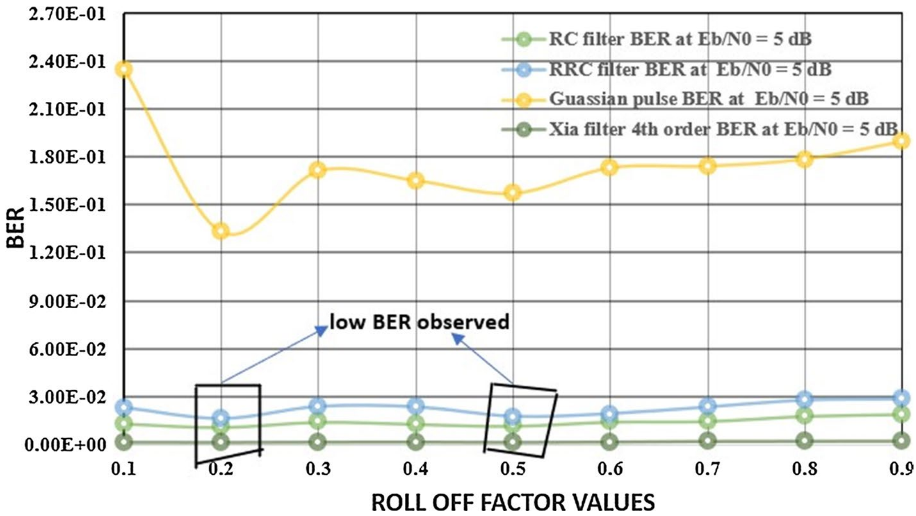

Fig. 19 BER analysis for roll-off factor values in prototype filters

Figure 19 and 20 shows the BER analysis, in which the GFDM system model is tested for different prototype filters such as RC, RRC, Gaussian, Xia 4th order filter. With the higher alpha values, the system's performance degrades, for low values of alpha, performance is not efficient. For two values of alpha 0.2 and 0.5, BER improvement is observed in all prototype filters. Hence, the two values are chosen for BER computation of GFDM system and channel coding techniques under both Guassian Noise and Rayleigh channels and USRP radio transceiver environment noise.

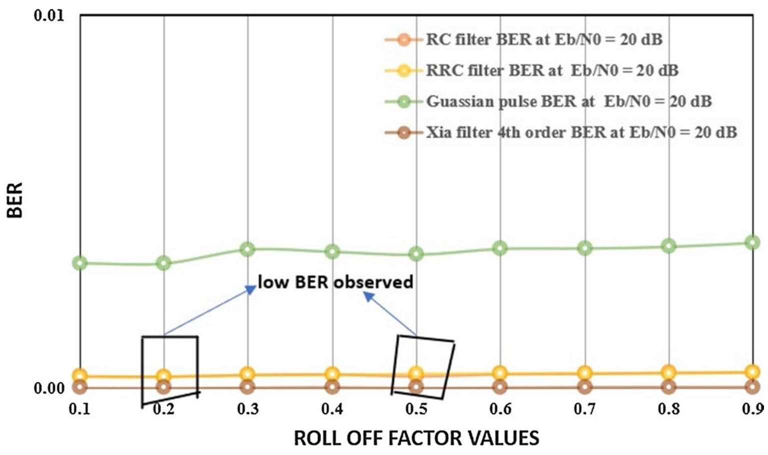

Fig. 20 BER analysis for the roll-off factor values in prototype filters

Figure 21 shows the GFDM out of band power is – 40 dB, and the OFDM signal's power is – 20 dB. Since less emission of band power is observed in GFDM, it is an essential candidate waveform for the fifth generation. Figure 21a is the OOB of Raised cosine filter characteristics with several symbols are 1920, and its OOB power is – 36 dB. Figure 21b shows RRC filter characteristics, and its OOB power is – 40 dB, hence in digital communication RRC filter is much prefer than RC filter. Figure 21c shows Xia 4^{th} order characteristics, the OOB value is – 37 dB, it is not preferable for spectrum, Fig. 21d shows Gaussian filter prototype filter characteristics, and its OOB is -28 dB.

Table 5 shows the USRP device results of convolutional coded GFDM system, the specifications are constraint length K is 15, and code rate r is ½.

The Parity check matrix of LDPC code is set as 256 × 512, the code rate of ½., maximum iterations of LDPC decoder is set to 30, 100, and 200 for the simulation results. All the BER values are computed from the NI RF hardware device called USRP 2901. Figures 22, 23, 24, 25, 26, 27, 28 and 29 shows the BER plots of values present in Tables 5, 6, 7, 8, 9, 10, 11, 12, 13, 14, 15. Figure 30 and 31 shows the BER plots of values present in Tables 16, 17, 18, 19.

Figure 22 shows BER analysis with SNR for AWGN channel, Raised cosine filter configuration with roll-off factor value 0.2, the PC-LDPC results at BER = 10^{-3} were 16 dB and 22 dB, respectively. The best value of SNR is 15 dB when two LDPC codes are connected in the parallel concatenation. The worst performance is seen in BCH coded GFDM system, i.e. BER = 10^{-2} were 21 dB respectively and convolutional coded GFDM has BER = 10^{-2} were 18 dB, Golay coded GFDM system has BER = 10^{-2} were 19 dB. The result is shown in Fig. 22 that PC-LDPC code outperforms LDPC code up to about 0.5 dB with RC pulse shaping filter.

Figure 23 shows BER analysis with SNR for the AWGN channel. The PC-LDPC results at BER = 10^{-4} were 24 dB and 21 dB, respectively. The best value of SNR is 16 dB for less BER value in PC-LDPC. The performance in BCH coded GFDM system is not efficient, i.e. BER = 10^{-2} were 18 dB respectively and convolutional coded GFDM has BER = 10^{-3} were 21 dB, Golay coded GFDM system has BER = 10^{-2} were 15 dB. The single LDPC codes have BER = 10^{-3} were 21 dB, and the PC LDPC code

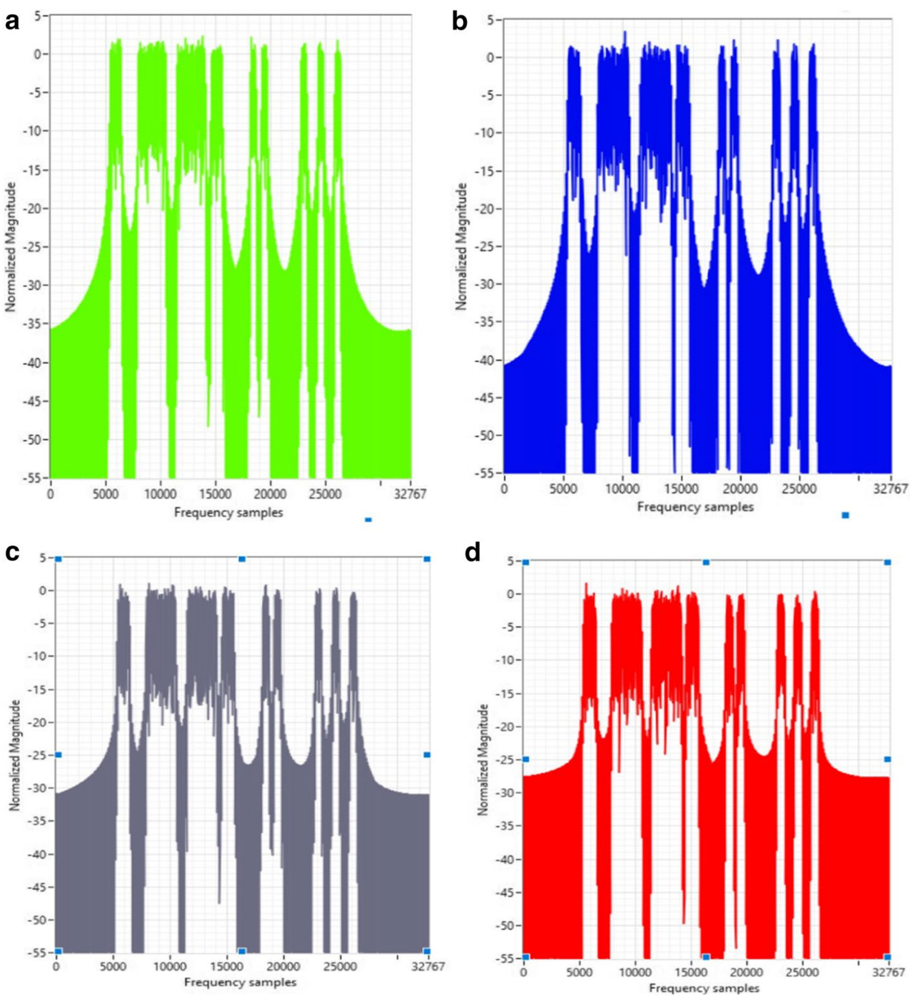

Fig. 21 Out of band emission performance of GFDM signal with RC, RRC, Guaasian, and Xia 4th order prototype filters are plotted

has BER = 10^{-3} were 20 dB. The result is shown in Fig. 23 that PC-LDPC code outperforms LDPC code with a coding gain of 1 dB.

The PC-LDPC code under the Rayleigh fading channel results at BER = 10^{-4} for 12 dB and 15 dB, respectively. The best value of SNR is 12 dB for less BER value in PC-LDPC. The BCH coded GFDM, Convolutional, Golay, single LDPC code system is not efficient, i.e., BER = 10^{-3} were 21 dB respectively. The result is shown in Fig. 24 that the PC-LDPC code of Rayleigh fading channel outperforms LDPC code up to about 6 dB with RRC pulse shaping filter with 0.2 as roll-off factor value.

The PC-LDPC code under Rayleigh fading channel results at BER = 10^{-4} were 15 dB, respectively. The best value of SNR is 15 dB for low BER value in PC-LDPC. The BCH coded GFDM, Convolutional, Golay, single LDPC code system is not efficient, i.e., BER = 10^{-2} were 18 dB respectively. The result is shown in Fig. 25 that the PC-LDPC

Table 5 BER computation of different prototype filters under the AWGN channel for Convolutional encoder and hard decision-based decoder of GFDM system (AWGN channel), with four types of prototype filters such as RC, RRC, Gaussian and Xia 4th order filter

S.No	Eb/N0	α = 0.2	α = 0.5	α = 0.2	α = 0.5	α = 0.2	α = 0.5	α = 0.2	α = 0.5
		Bit Error Rate for RC prototype filter		Bit Error Rate for RRC prototype filter		Bit Error Rate for Gaussian prototype filter		Bit Error Rate for Xia 4th order prototype filter	
1	[1–3]	5.25xE-1	5.13xE-1	5.31xE-1	5.09xE-1	5.98xE-1	5.87xE-1	3.29xE-1	3.19xE-1
2	[3–6]	4.87xE-1	4.72xE-1	4.72xE-1	4.65xE-1	5.43xE-1	5.12xE-1	2.85xE-1	2.95xE-1
3	[6–9]	4.65xE-1	4.55xE-1	4.54xE-1	4.43xE-1	5.13xE-1	4.97xE-1	2.95xE-1	2.88xE-1
4	[9–12]	4.78xE-1	4.39xE-1	4.61xE-1	4.12xE-1	5.09xE-1	4.86xE-1	2.82xE-1	2.75xE-1
5	[12–15]	4.62xE-1	4.72xE-1	4.54xE-1	4.52xE-1	4.98xE-1	5.21xE-1	2.95xE-1	2.85xE-1
6	[15–18]	3.72xE-1	3.51xE-1	3.51xE-1	3.19xE-1	4.54xE-1	4.92xE-1	2.62xE-2	2.51xE-2
7	[18–21]	4.30xE-2	4.72xE-2	4.19xE-2	4.54xE-2	4.87xE-2	5.32xE-2	3.19xE-2	2.95xE-2
8	[21–24]	4.13xE-2	5.13xE-2	3.98xE-2	4.92xE-2	4.23xE-2	5.81xE-2	3.04xE-2	3.14xE-3
9	[24–27]	4.42xE-2	4.61xE-2	4.00xE-2	4.11xE-2	4.12xE-2	5.23xE-2	2.95xE-3	2.64xE-3
10	[27–30]	4.82xE-3	4.93xE-3	4.65xE-3	4.29xE-3	5.12xE-3	5.32xE-3	2.91xE-3	2.51xE-3

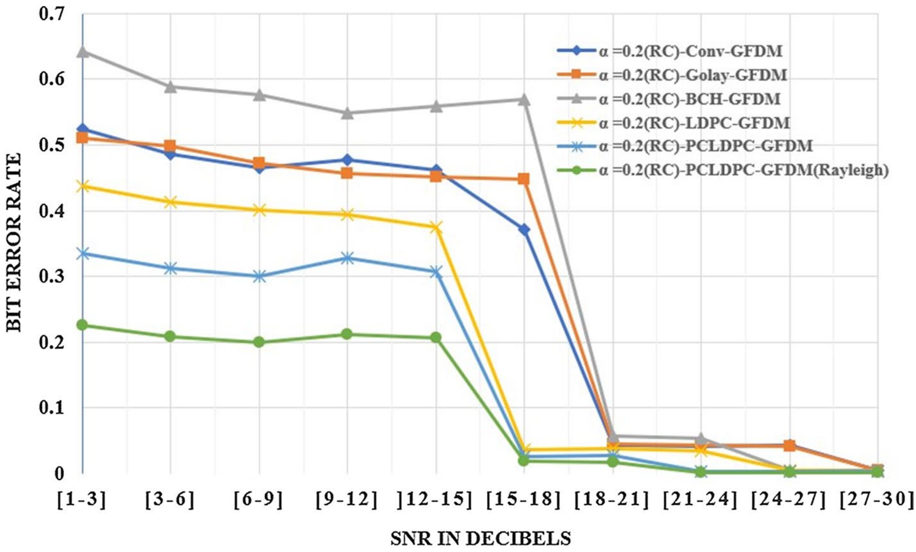

Fig. 22 BER analysis of different channel coded GFDM system under AWGN channel, and PC-LDPC-GFDM system with frequency-selective Rayleigh channel for RC prototype filter only with roll-off factor value 0.2

code of Rayleigh fading channel outperforms LDPC code up to about 3 dB with RRC pulse shaping filter with 0.5 as roll-off factor value.

The PC-LDPC code under Rayleigh fading channel results at BER = 10^{-3} were 15 dB, respectively. The best value of SNR is 18 dB for less BER value in PC-LDPC. The performance in BCH coded GFDM, Convolutional, Golay, single LDPC code system is not efficient, i.e., BER = 10^{-2} were 15 dB, respectively. The performance of all the channel coding

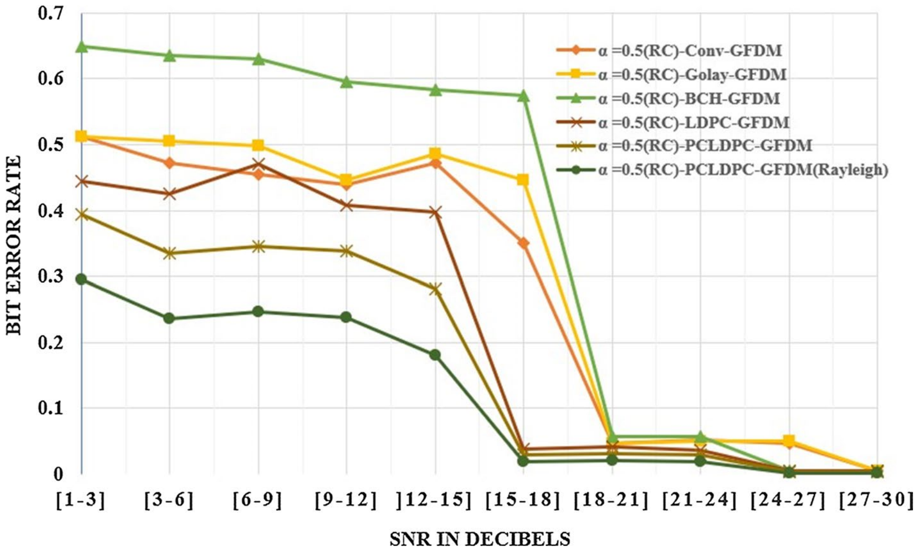

Fig. 23 BER analysis of RC pulse shaped filter with roll-off factor value 0.5 for different channel coded GFDM system under AWGN channel, and PC-LDPC-GFDM system with frequency-selective Rayleigh channel

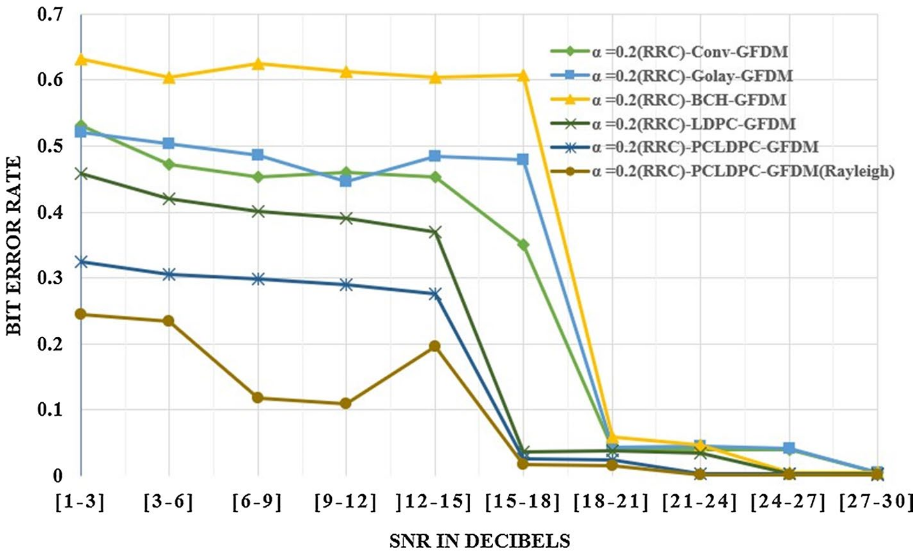

Fig. 24 BER analysis of RRC prototype filter based different channel coded GFDM system under AWGN channel, and PC-LDPC-GFDM system with frequency-selective Rayleigh channel with roll-off factor value 0.2

schemes is the same for high SNR values. The result is shown in Fig. 26 that the PC-LDPC code of the Rayleigh fading channel outperforms LDPC code up to about 0.7 dB with a Gaussian filter with 0.2 as a roll-off factor value.

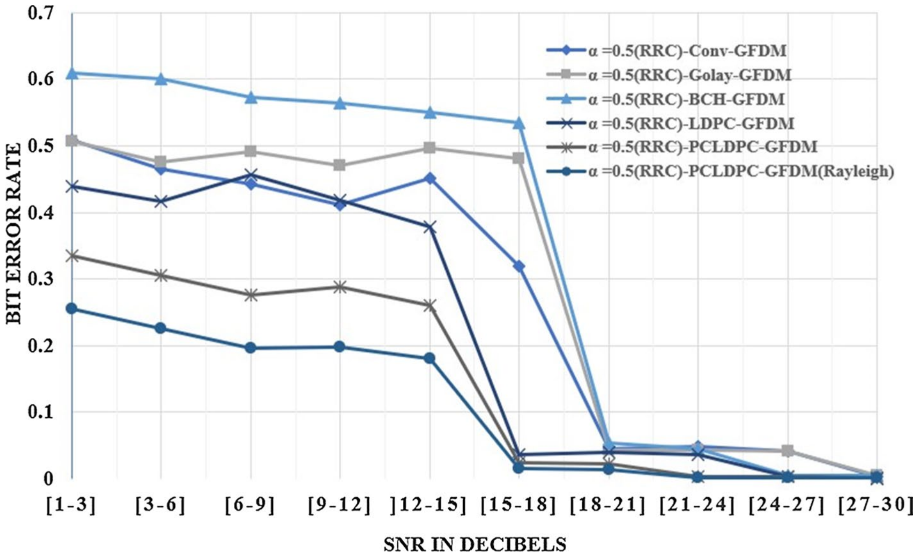

Fig. 25 BER analysis of channel coded GFDM system under AWGN channel, and PC-LDPC-GFDM system with frequency-selective Rayleigh channel for RRC prototype filter only with roll-off factor value 0.5

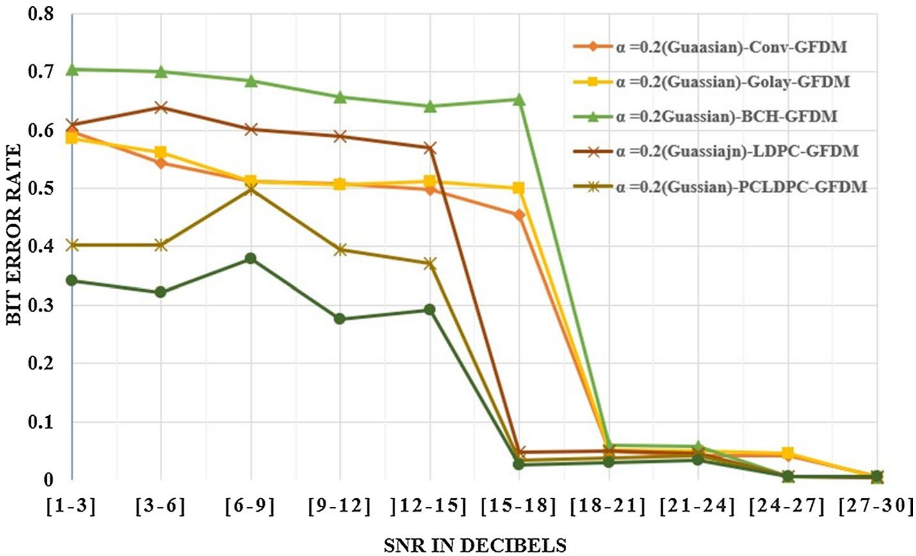

Fig. 26 BER analysis of Gaussian prototype filter-based channel coded GFDM system under AWGN channel, and PC-LDPC-GFDM system with frequency-selective Rayleigh channel with roll-off factor value 0.2

The LDPC code under AWGN channel results at BER = 10^{-4} was 15 dB respectively. The best value of SNR is 15 dB for less BER value in LDPC. BCH coded GFDM, Convolutional, Golay, single LDPC code system is not efficient, i.e., BER = 10^{-3} were 21 dB respectively. The result is shown in Fig. 27 that the LDPC code of the Gaussian channel outperforms the PC-LDPC code up to about 2.5 dB.

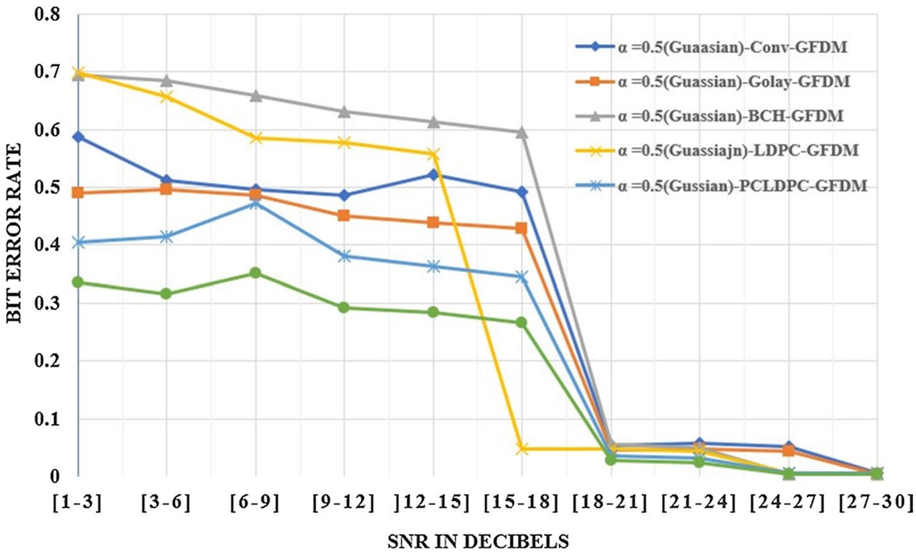

Fig. 27 BER analysis of channel coded GFDM system under AWGN channel, and PC-LDPC-GFDM system with frequency-selective Rayleigh channel for Gaussian prototype filter only with roll-off factor value 0.5

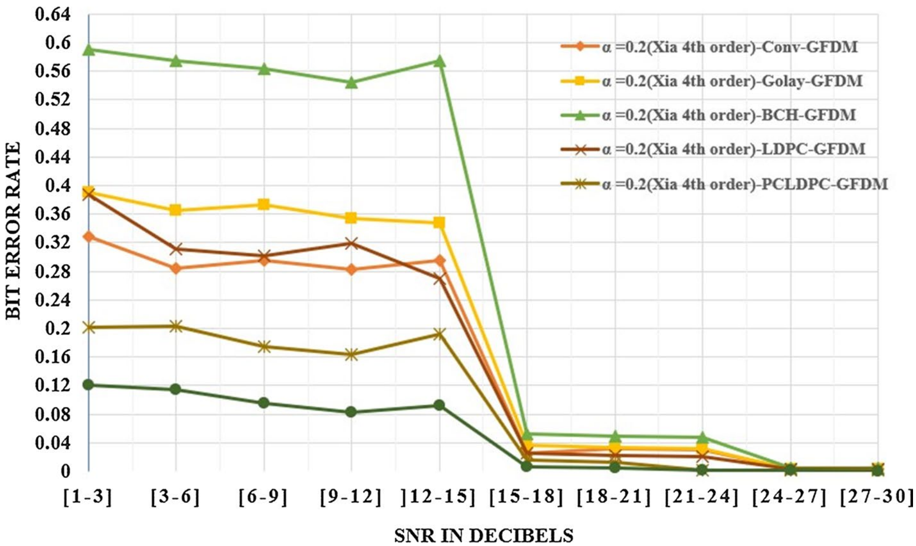

Fig. 28 BER analysis of Xia 4^{th} order filter for roll-off factor value 0.2 based channel coded GFDM system under AWGN channel, and PC-LDPC coded GFDM system with frequency-selective Rayleigh channel

The PC-LDPC code under Rayleigh fading channel results at BER = 10^{-4} were 12 dB respectively. The best value of SNR is 12 dB for less BER value in PC-LDPC. The BCH coded GFDM, Convolutional, Golay, single LDPC code system is not efficient, i.e., BER = 10^{-3} were 21 dB, respectively, the BCH coded GFDM has worst BER performance

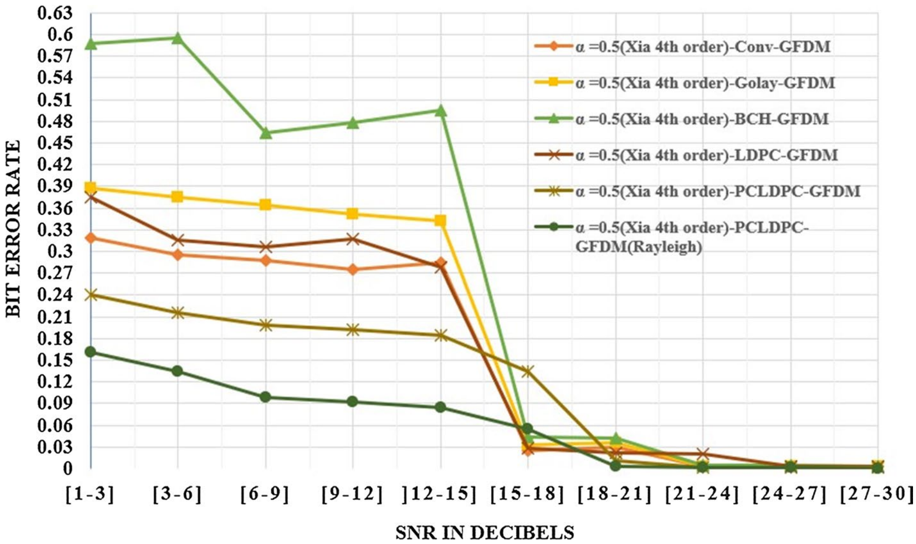

Fig. 29 BER analysis of channel coded GFDM system under AWGN channel, and PC-LDPC-GFDM system with frequency-selective Rayleigh channel for Xia 4th order prototype filter only with roll-off factor value 0.5

Table 6 BER computation of different prototype filters under AWGN channel for Golay coded GFDM system

S.No	Eb/N0	α = 0.2	α = 0.5	α = 0.2	α = 0.5	α = 0.2	α = 0.5	α = 0.2	α = 0.5
		Bit Error Rate for RC prototype filter		Bit Error Rate for RRC prototype filter		Bit Error Rate for Gaussian prototype filter		Bit Error Rate for Xia 4th order prototype filter	
1	[1–3]	5.11xE-1	5.12xE-1	5.21xE-1	5.07xE-1	5.86xE-1	4.91xE-1	3.90xE-1	3.87xE-1
2	[3–6]	4.98xE-1	5.06xE-1	5.04xE-1	4.75xE-1	5.61xE-1	4.96xE-1	3.65xE-1	3.75xE-1
3	[6–9]	4.73xE-1	4.98xE-1	4.86xE-1	4.92xE-1	5.13xE-1	4.87xE-1	3.73xE-1	3.64xE-1
4	[9–12]	4.56xE-1	4.46xE-1	4.46xE-1	4.71xE-1	5.06xE-1	4.51xE-1	3.54xE-1	3.51xE-1
5	[12–15]	4.51xE-1	4.86xE-1	4.85xE-1	4.97xE-1	5.12xE-1	4.38xE-1	3.48xE-1	3.43xE-1
6	[15–18]	4.48xE-1	4.46xE-1	4.79xE-1	4.81xE-1	5.01xE-1	4.29xE-1	3.65xE-2	3.33xE-2
7	[18–21]	4.59xE-2	4.65xE-2	4.36xE-2	4.36xE-2	5.08xE-2	4.56xE-2	3.38xE-2	3.54xE-2
8	[21–24]	4.35xE-2	5.01xE-2	4.48xE-2	4.28xE-2	4.95xE-2	4.81xE-2	3.12xE-2	3.21xE-3
9	[24–27]	4.23xE-2	4.96xE-2	4.21xE-2	4.18xE-2	4.65xE-2	4.47xE-2	3.09xE-3	3.85xE-3
10	[27–30]	4.67xE-3	4.79xE-3	4.55xE-3	4.45xE-3	4.91xE-3	4.37xE-3	3.55xE-3	3.45xE-3

The specifications of Golay codes are (23, 12, 3), i.e. (n,k,t), n is the codeword length, k is data word length, t is error-correcting capability

for SNR below 18 dB values. The result is shown in Fig. 28 that the PC-LDPC code of Xia 4th order filter under Rayleigh fading channel outperforms PC-LDPC code under the AWGN channel up to about 3 dB.

The LDPC code under AWGN channel results at BER = 10^{-4} was 15 dB respectively. The best value of SNR is 15 dB for less BER value in LDPC. The performance in BCH

Table 7 BER computation of different prototype filters under the AWGN channel for BCH coded GFDM system, BCH code specifications are (63,36,5), (n,k,t)

S.No	Eb/N0	α = 0.2	α = 0.5	α = 0.2	α = 0.5	α = 0.2	α = 0.5	α = 0.2	α = 0.5
		Bit Error Rate for RC prototype filter		Bit Error Rate for RRC prototype filter		Bit Error Rate for Gaussian prototype filter		Bit Error Rate for Xia 4th order prototype filter	
1	[1–3]	6.42xE-1	6.50xE-1	6.32xE-1	6.10xE-1	7.05xE-1	6.95xE-1	5.90xE-1	5.87xE-1
2	[3–6]	5.89xE-1	6.36xE-1	6.05xE-1	6.00xE-1	7.00xE-1	6.85xE-1	5.75xE-1	5.95xE-1
3	[6–9]	5.76xE-1	6.31xE-1	6.25xE-1	5.73xE-1	6.85xE-1	6.58xE-1	5.63xE-1	4.64xE-1
4	[9–12]	5.49xE-1	5.95xE-1	6.13xE-1	5.64xE-1	6.56xE-1	6.32xE-1	5.45xE-1	4.78xE-1
5	[12–15]	5.59xE-1	5.84xE-1	6.05xE-1	5.51xE-1	6.41xE-1	6.13xE-1	5.75xE-1	4.95xE-1
6	[15–18]	5.69xE-1	5.75xE-1	6.07xE-1	5.35xE-1	6.52xE-1	5.95xE-1	5.32xE-2	4.35xE-2
7	[18–21]	5.76xE-2	5.74xE-2	5.91xE-2	5.45xE-2	5.95xE-2	5.65xE-2	4.95xE-2	4.21xE-2
8	[21–24]	5.45xE-2	5.65xE-2	4.75xE-2	4.47xE-2	5.74xE-2	5.05xE-2	4.75xE-2	4.01xE-3
9	[24–27]	4.97xE-3	5.01xE-3	4.91xE-3	5.15xE-3	5.50xE-3	4.95xE-3	4.34xE-3	3.99xE-3
10	[27–30]	4.58xE-3	4.47xE-3	4.65xE-3	5.95xE-3	4.91xE-3	4.39xE-3	4.21xE-3	3.55xE-3

The systematic decoder is used, compare to a systematic decoder, the non-systematic decoder is not preferred because its performance is not efficient

Table 8 BER computation of Raised cosine prototype filters under AWGN channel for single long length high complexity LDPC encoder and decoder

S.No	Eb/No	α = 0.2			α = 0.5		
		Maximum iterations for the decoder (MaxIT)					
		30	100	200	30	100	200
1	[1–3]	4.37xE-1	3.98xE-1	3.75xE-2	4.45xE-1	3.99xE-1	3.81xE-2
2	[3–6]	4.13xE-1	3.84xE-1	3.54xE-2	4.26xE-1	3.83xE-1	3.68xE-2
3	[6–9]	4.02xE-1	3.78xE-1	3.12xE-2	4.71xE-1	3.76xE-1	3.24xE-2
4	[9–12]	3.95xE-1	3.65xE-1	2.95xE-2	4.08xE-1	3.72xE-1	2.98xE-2
5	[12–15]	3.75xE-1	3.98xE-1	2.20xE-3	3.98xE-1	3.97xE-1	2.35xE-3
6	[15–18]	3.69xE-2	3.55xE-2	2.87xE-3	3.78xE-2	3.49xE-2	2.76xE-3
7	[18–21]	3.77xE-2	3.43xE-2	2.57xE-3	4.12xE-2	3.53xE-2	3.12xE-3
8	[21–24]	3.55xE-2	3.19xE-2	4.12xE-4	3.69xE-2	3.50xE-2	3.89xE-4
9	[24–27]	4.59xE-3	4.12xE-3	4.57xE-4	4.52xE-3	4.03xE-3	2.57xE-5
10	[27–30]	4.23xE-3	4.02xE-4	4.99xE-5	5.12xE-4	3.93xE-4	2.87xE-5

coded GFDM, Convolutional, Golay, single LDPC code system is not efficient, i.e., BER = 10^{-2} were 21 dB respectively The result is shown in Fig. 29 that LDPC code under AWGN channel outperforms PC-LDPC code up to about 2 dB.

The PC-LDPC decoder maximum iterations are kept as 100 and 200. For different pulse shaping filters such as RC, RRC, and Gaussian, Xia 4th order filters are tested with maximum iterations. BER = 10^{-5} was SNR = 10 dB is observed for Xia filter, with Maximum iterations kept as 200. The remaining prototype filters with roll-off factor value 0.5 provides BER = 10^{-4} were SNR = 18 dB, the coding gain of 6.5 dB is observed

Table 9 BER computation of Root Raised Cosine prototype filter under AWGN channel for single long length high complexity LDPC encoder and decoder

S.No	Eb/No	α = 0.2			α = 0.5		
		Maximum iterations for the decoder (MaxIT)					
		30	100	200	30	100	200
1	[1–3]	4.58xE-1	4.08xE-1	4.12xE-2	4.39xE-1	4.10xE-1	3.85xE-2
2	[3–6]	4.20xE-1	3.98xE-1	3.75xE-2	4.16xE-1	3.9xE-1	3.58xE-2
3	[6–9]	4.01xE-1	3.89xE-1	3.08xE-2	4.56xE-1	3.87xE-1	3.40xE-2
4	[9–12]	3.90xE-1	3.75xE-1	2.90xE-2	4.18xE-1	3.65xE-1	3.05xE-2
5	[12–15]	3.70xE-1	3.87xE-1	2.25xE-3	3.78xE-1	3.80xE-1	2.12xE-3
6	[15–18]	3.65xE-2	3.45xE-2	2.65xE-3	3.65xE-2	3.40xE-2	2.71xE-3
7	[18–21]	3.87xE-2	3.33xE-2	2.57xE-3	4.00xE-2	3.33xE-2	3.01xE-3
8	[21–24]	3.51xE-2	3.05xE-2	3.20xE-4	3.59xE-2	3.50xE-2	3.85xE-4
9	[24–27]	4.00xE-3	3.65xE-3	4.05xE-4	3.95xE-3	3.99xE-3	2.47xE-5
10	[27–30]	3.95xE-3	3.87xE-4	3.95xE-5	5.00xE-4	3.81xE-4	2.67xE-5

Table 10 BER computation of Gaussian prototype filter under AWGN channel for single long length high complexity LDPC encoder and decoder

S.No	Eb/No	α = 0.2			α = 0.5		
		Maximum iterations for the decoder (MaxIT)					
		30	100	200	30	100	200
1	[1–3]	6.09xE-1	6.08xE-1	5.90xE-2	6.98xE-1	6.01xE-1	5.65xE-2
2	[3–6]	6.39xE-1	5.98xE-1	5.45xE-2	6.56xE-1	5.87xE-1	5.38xE-2
3	[6–9]	6.01xE-1	5.89xE-1	5.08xE-2	5.86xE-1	5.67xE-1	4.80xE-2
4	[9–12]	5.89xE-1	5.75xE-1	3.90xE-2	5.78xE-1	5.55xE-1	4.05xE-2
5	[12–15]	5.70xE-1	5.87xE-1	3.25xE-3	5.58xE-1	5.60xE-1	3.52xE-3
6	[15–18]	4.69xE-2	5.45xE-2	3.05xE-3	4.85xE-2	5.20xE-2	3.11xE-3
7	[18–21]	4.87xE-2	4.73xE-2	4.00xE-3	4.76xE-2	4.38xE-2	3.81xE-3
8	[21–24]	4.61xE-2	4.53xE-2	3.10xE-4	4.39xE-2	4.10xE-2	3.95xE-4
9	[24–27]	5.10xE-3	4.45xE-3	2.90xE-4	5.15xE-3	4.79xE-3	3.47xE-4
10	[27–30]	4.95xE-3	4.57xE-3	3.87xE-4	5.00xE-3	4.20xE-3	3.10xE-5

in PC-LDPC codes with Xia 4th order corresponding to PC-LDPC codes for other prototype filters.

The PC-LDPC decoder maximum iterations are kept as 100 and 200. For different prototype filters such as RC, RRC, and Gaussian, Xia 4th order filters are tested with maximum iterations. BER = 10^{-5} was SNR of 9 dB is observed for Xia filter, with Maximum iterations kept as 200. PC-LDPC-GFDM system in the combination of Xia prototype filter with roll-off factor value 0.5 outperforms other PC-LDPC-GFDM of RC, RRC, Gaussian filters with a coding gain of 3 dB.

Table 11 BER computation of Xia 4th order prototype filter under AWGN channel for single long length high complexity LDPC encoder and decoder

S.No	Eb/No	α = 0.2			α = 0.5		
		Maximum iterations for the decoder(MaxIT)					
		30	100	200	30	100	200
1	[1–3]	3.88xE-1	3.08xE-1	3.21xE-2	3.75xE-1	2.95xE-1	2.25xE-2
2	[3–6]	3.11xE-1	3.68xE-1	3.10xE-2	3.16xE-1	3.57xE-1	2.18xE-2
3	[6–9]	3.01xE-1	3.18xE-1	2.95xE-2	3.06xE-1	3.17xE-1	2.08xE-2
4	[9–12]	3.19xE-1	3.15xE-1	2.75xE-2	3.18xE-1	3.15xE-1	2.05xE-2
5	[12–15]	2.70xE-1	2.98xE-1	2.00xE-3	2.78xE-1	2.78xE-1	3.98xE-3
6	[15–18]	2.61xE-2	2.45xE-2	2.85xE-3	2.75xE-2	2.35xE-2	2.5xE-3
7	[18–21]	2.27xE-2	2.19xE-2	3.15xE-3	2.16xE-2	2.15xE-2	2.81xE-3
8	[21–24]	2.11xE-2	3.98xE-3	3.12xE-4	2.09xE-2	2.95xE-3	2.75xE-4
9	[24–27]	3.91xE-3	3.12xE-3	3.50xE-4	3.50xE-3	2.75xE-3	2.61xE-4
10	[27–30]	3.25xE-3	3.02xE-4	3.97xE-5	3.10xE-3	2.50xE-4	2.10xE-5

Table 12 BER computation of Raised Cosine prototype filter under AWGN channel based Parallel concatenation of LDPC decoder

S.No	Eb/No	α = 0.2			α = 0.5		
		Maximum Iterations for Decoder (MaxIT)					
		30	100	200	30	100	200
1	[1–3]	3.35xE-1	3.01xE-1	2.95xE-2	3.95xE-1	3.25xE-1	4.15xE-2
2	[3–6]	3.13xE-1	3.08xE-1	2.75xE-2	3.36xE-1	3.15xE-1	3.10xE-2
3	[6–9]	3.00xE-1	2.78xE-1	2.19xE-2	3.46xE-1	3.10xE-1	2.98xE-2
4	[9–12]	3.28xE-1	2.65xE-1	2.15xE-2	3.38xE-1	2.75xE-1	2.15xE-2
5	[12–15]	3.07xE-1	2.90xE-1	2.01xE-3	2.81xE-1	2.95xE-1	2.05xE-3
6	[15–18]	2.61xE-2	2.65xE-2	2.25xE-3	2.95xE-2	2.89xE-2	2.10xE-3
7	[18–21]	2.72xE-2	2.63xE-2	2.11xE-3	3.15xE-2	2.51xE-2	2.15xE-3
8	[21–24]	3.21xE-3	2.25xE-3	3.92xE-4	2.95xE-2	2.20xE-3	2.91xE-4
9	[24–27]	3.01xE-3	3.28xE-3	4.50xE-4	2.71xE-3	3.15xE-3	4.11xE-5
10	[27–30]	2.95xE-3	3.02xE-3	4.27xE-5	3.10xE-3	2.50xE-3	3.75xE-5

Figure 32 shows the BER analysis of PC-LDPC codes in an OFDM system compared with a single LDPC code. This Fig. shows BER analysis with SNR for AWGN channel, RC pulse filter configuration with α = 0.52 the LDPC code under AWGN channel results at BER = 10^{-3} was 5 dB respectively. The best value of SNR is 8 dB for less BER value in PC-LDPC. The result is shown in Fig. 31 that the PC-LDPC code outperforms the LDPC code with a coding gain of 2 dB.

Table 13 BER computation of Root Raised Cosine prototype filter under AWGN channel based Parallel concatenation of LDPC decoder

S.No	Eb/No	α = 0.2			α = 0.5		
		Maximum Iterations for Decoder (MaxIT)					
		30	100	200	30	100	200
1	[1–3]	3.25xE-1	2.90xE-1	2.75xE-2	3.35xE-1	2.75xE-1	2.15xE-2
2	[3–6]	3.05xE-1	2.81xE-1	2.63xE-2	3.06xE-1	2.65xE-1	2.54xE-2
3	[6–9]	2.99xE-1	2.70xE-1	2.10xE-2	2.76xE-1	2.50xE-1	2.08xE-2
4	[9–12]	2.90xE-1	2.65xE-1	2.25xE-2	2.88xE-1	2.35xE-1	2.13xE-2
5	[12–15]	2.77xE-1	2.80xE-1	2.61xE-3	2.61xE-1	2.45xE-1	2.40xE-3
6	[15–18]	2.58xE-2	2.75xE-2	2.25xE-3	2.45xE-2	2.39xE-2	2.12xE-3
7	[18–21]	2.36xE-2	2.43xE-2	2.05xE-3	2.18xE-2	2.21xE-2	2.00xE-3
8	[21–24]	3.1xE-3	2.15xE-3	3.52xE-4	2.95xE-3	2.05xE-3	3.00xE-4
9	[24–27]	2.80xE-3	2.48xE-3	4.30xE-4	2.71xE-3	2.75xE-3	4.11xE-5
10	[27–30]	2.61xE-3	2.08xE-3	4.10xE-5	2.50xE-3	2.40xE-3	3.85xE-5

Table 14 BER computation of Guassian prototype filter under AWGN channel based Parallel concatenation of LDPC decoder

S.No	Eb/No	α = 0.2			α = 0.5		
		Maximum iterations for the decoder (MaxIT)					
		30	100	200	30	100	200
1	[1–3]	4.02xE-1	4.15xE-1	3.95xE-2	4.05xE-1	4.25xE-1	3.75xE-2
2	[3–6]	4.02xE-1	4.96xE-1	3.65xE-2	4.15xE-1	4.85xE-1	3.68xE-2
3	[6–9]	4.99xE-1	4.83xE-1	3.10xE-2	4.72xE-1	4.73xE-1	2.98xE-2
4	[9–12]	3.95xE-1	4.73xE-1	3.20xE-2	3.82xE-1	4.64xE-1	3.12xE-2
5	[12–15]	3.72xE-1	4.82xE-1	3.15xE-2	3.64xE-1	4.72xE-1	3.05xE-3
6	[15–18]	3.45xE-2	4.41xE-2	3.00xE-2	3.45xE-1	4.30xE-2	2.95xE-3
7	[18–21]	3.81xE-2	3.73xE-2	4.10xE-3	3.65xE-2	3.51xE-2	5.90xE-3
8	[21–24]	4.11xE-2	3.55xE-2	4.19xE-4	3.10xE-2	3.40xE-2	3.95xE-4
9	[24–27]	6.00xE-3	3.40xE-2	3.89xE-4	5.90xE-3	3.25xE-2	3.72xE-4
10	[27–30]	6.51xE-3	3.50xE-3	3.80xE-4	5.50xE-3	3.15xE-3	3.45xE-4

Table 15 BER computation of Xia 4th order prototype filter under AWGN channel based Parallel concatenation of LDPC decoder

S.No	Eb/No	α = 0.2			α = 0.5		
		Maximum Iterations for Decoder (MaxIT)					
		30	100	200	30	100	200
1	[1–3]	2.01xE-1	2.15xE-1	1.95xE-2	2.41xE-1	2.14xE-1	1.62xE-2
2	[3–6]	2.04xE-1	1.90xE-1	1.65xE-2	2.15xE-1	1.65xE-1	1.35xE-2
3	[6–9]	1.75xE-1	1.85xE-1	1.20xE-2	1.98xE-1	1.54xE-1	1.10xE-2
4	[9–12]	1.63xE-1	1.75xE-1	1.18xE-2	1.92xE-1	1.32xE-1	1.14xE-2
5	[12–15]	1.92xE-1	1.62xE-1	1.51xE-2	1.85xE-1	1.42xE-1	1.45xE-3
6	[15–18]	1.52xE-2	1.51xE-2	1.30xE-2	1.35xE-1	1.25xE-2	1.25xE-3
7	[18–21]	1.32xE-2	1.33xE-2	1.20xE-3	1.15xE-2	1.15xE-2	1.10xE-4
8	[21–24]	2.10xE-3	1.25xE-2	1.10xE-4	2.05xE-3	1.12xE-3	0.95xE-4
9	[24–27]	1.92xE-3	1.40xE-2	2.00xE-5	1.75xE-3	1.24xE-3	1.15xE-5
10	[27–30]	1.69xE-3	1.00xE-3	2.20xE-5	1.35xE-3	0.54xE-3	1.25xE-5

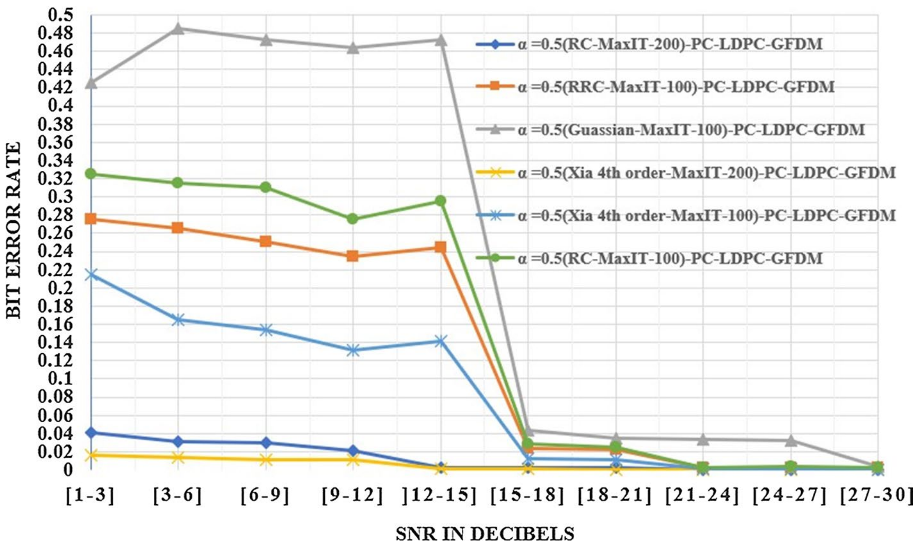

Fig. 30 BER analysis of under AWGN channel, and frequency-selective Rayleigh channel for RC, RRC, Gaussian and Xia 4th order prototype filters with roll-off factor value 0.5., and the MaxIT represents the maximum number of iterations in the decoder

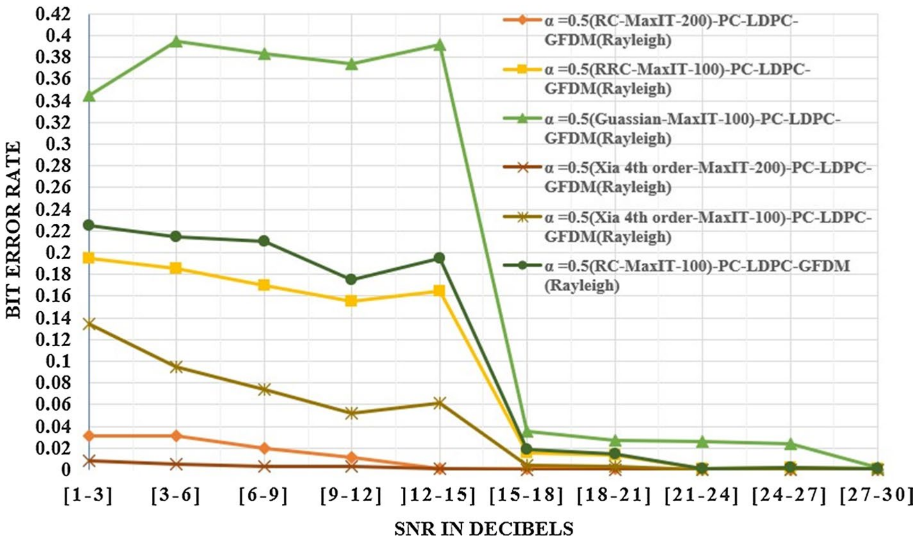

Fig. 31 BER analysis of PC-LDPC coded GFDM system with frequency-selective Rayleigh fading channel for RC, RRC, Gaussian, and Xia 4th order prototype filters with roll-off factor value 0.5., the MaxIT represents a maximum number of iterations in the decoder

Table 16 BER computation of Parallel concatenation of LDPC decoder, serial scheduling/message-passing algorithm is used in decoder section, with Raised Cosine prototype filter under Rayleigh Fading channel (Jakes model)

S.No	Eb/No	α = 0.2			α = 0.5		
		Maximum Iterations for Decoder (MaxIT)					
		30	100	200	30	100	200
1	[1–3]	2.25xE-1	2.01xE-1	1.95xE-2	2.95xE-1	2.25xE-1	3.15xE-2
2	[3–6]	2.09xE-1	2.08xE-1	1.75xE-2	2.36xE-1	2.15xE-1	3.10xE-2
3	[6–9]	2.00xE-1	1.87xE-1	1.19xE-2	2.46xE-1	2.10xE-1	1.98xE-2
4	[9–12]	2.12xE-1	1.69xE-1	1.15xE-2	2.38xE-1	1.75xE-1	1.15xE-2
5	[12–15]	2.07xE-1	1.97xE-1	1.01xE-3	1.81xE-1	1.95xE-1	1.05xE-3
6	[15–18]	1.95xE-2	1.75xE-2	1.25xE-3	1.95xE-2	1.89xE-2	1.10xE-3
7	[18–21]	1.79xE-2	1.53xE-2	1.11xE-3	2.15xE-2	1.51xE-2	1.15xE-3
8	[21–24]	2.18xE-3	1.65xE-3	2.92xE-4	1.95xE-2	1.20xE-3	1.91xE-4
9	[24–27]	2.01xE-3	2.21xE-3	3.50xE-4	1.71xE-3	2.15xE-3	3.11xE-5
10	[27–30]	1.92xE-3	2.08xE-3	3.27xE-5	2.10xE-3	1.50xE-3	2.75xE-5

Table 17 BER computation of Parallel concatenation of LDPC decoder, with serial scheduling/message-passing algorithm, is used as a decoder section, with Root Raised Cosine prototype filter under Rayleigh Fading channel (Jakes model) is used as configuration

S.No	Eb/No	α = 0.2			α = 0.5		
		Maximum Iterations for Decoder (MaxIT)					
		30	100	200	30	100	200
1	[1–3]	2.45xE-1	1.93xE-1	1.95xE-2	2.55xE-1	1.95xE-1	1.35xE-2
2	[3–6]	2.35xE-1	1.91xE-1	1.73xE-2	2.26xE-1	1.85xE-1	1.74xE-2
3	[6–9]	1.19xE-1	1.83xE-1	1.20xE-2	1.96xE-1	1.70xE-1	1.38xE-2
4	[9–12]	1.10xE-1	1.75xE-1	1.35xE-2	1.98xE-1	1.55xE-1	1.33xE-2
5	[12–15]	1.97xE-1	1.60xE-1	1.81xE-3	1.81xE-1	1.65xE-1	1.60xE-3
6	[15–18]	1.78xE-2	1.55xE-2	1.55xE-3	1.65xE-2	1.59xE-2	1.32xE-3
7	[18–21]	1.56xE-2	1.33xE-2	1.35xE-3	1.38xE-2	1.31xE-2	1.30xE-3
8	[21–24]	2.32xE-3	1.25xE-3	2.72xE-4	1.35xE-3	1.25xE-3	2.20xE-4
9	[24–27]	1.10xE-3	1.28xE-3	3.20xE-4	1.91xE-3	1.95xE-3	3.31xE-5
10	[27–30]	1.81xE-3	1.18xE-3	3.30xE-5	1.70xE-3	1.60xE-3	2.95xE-5

Table 18 BER computation of different prototype filters of Parallel concatenation of LDPC decoder, with serial scheduling/message-passing algorithm, is used as a decoder section, with Gaussian prototype filter under Rayleigh Fading channel (Jakes model) is used as configuration

S.No	Eb/No	α = 0.2			α = 0.5		
		Maximum Iterations for Decoder (MaxIT)					
		30	100	200	30	100	200
1	[1–3]	3.42xE-1	3.35xE-1	2.75xE-2	3.35xE-1	3.45xE-1	2.85xE-2
2	[3–6]	3.22xE-1	3.76xE-1	2.55xE-2	3.15xE-1	3.95xE-1	2.78xE-2
3	[6–9]	3.79xE-1	3.93xE-1	2.30xE-2	3.52xE-1	3.83xE-1	1.68xE-2
4	[9–12]	2.75xE-1	3.87xE-1	2.20xE-2	2.92xE-1	3.74xE-1	2.32xE-2
5	[12–15]	2.92xE-1	3.72xE-1	2.15xE-2	2.84xE-1	3.92xE-1	1.45xE-3
6	[15–18]	2.65xE-2	3.61xE-2	2.00xE-2	2.65xE-1	3.50xE-2	1.75xE-3
7	[18–21]	2.91xE-2	2.93xE-2	3.10xE-3	2.75xE-2	2.71xE-2	4.30xE-3
8	[21–24]	3.31xE-2	2.75xE-2	3.19xE-4	2.40xE-2	2.60xE-2	2.75xE-4
9	[24–27]	5.30xE-3	2.60xE-2	2.89xE-4	4.72xE-3	2.45xE-2	1.92xE-4
10	[27–30]	5.71xE-3	2.70xE-3	2.80xE-4	4.69xE-3	2.35xE-3	2.55xE-4

Table 19 BER computation of Parallel concatenation of LDPC decoder, serial scheduling/message-passing algorithm is used as decoder section, with Xia 4th order prototype filter under Rayleigh Fading channel (Jakes model) is used as configuration

S.No	Eb/No	α = 0.2			α = 0.5		
		Maximum Iterations for Decoder (MaxIT)					
		30	100	200	30	100	200
1	[1–3]	1.21xE-1	1.35xE-1	0.95xE-2	1.61xE-1	1.34xE-1	0.82xE-2
2	[3–6]	1.14xE-1	0.90xE-1	0.75xE-2	1.35xE-1	0.95xE-1	0.55xE-2
3	[6–9]	0.95xE-1	0.95xE-1	0.40xE-2	0.98xE-1	0.74xE-1	0.30xE-2
4	[9–12]	0.83xE-1	0.85xE-1	0.28xE-2	0.92xE-1	0.52xE-1	0.34xE-2
5	[12–15]	0.92xE-1	0.72xE-1	0.71xE-2	0.85xE-1	0.62xE-1	0.65xE-3
6	[15–18]	0.72xE-2	0.71xE-2	0.50xE-2	0.55xE-1	0.45xE-2	0.45xE-3
7	[18–21]	0.52xE-2	0.53xE-2	0.40xE-3	0.35xE-2	0.35xE-2	0.30xE-4
8	[21–24]	1.30xE-3	0.45xE-2	0.30xE-4	1.35xE-3	0.32xE-3	0.75xE-4
9	[24–27]	0.92xE-3	0.60xE-2	1.20xE-5	0.95xE-3	0.44xE-3	0.35xE-5
10	[27–30]	0.79xE-3	0.40xE-3	1.40xE-5	0.55xE-3	0.34xE-3	0.45xE-5

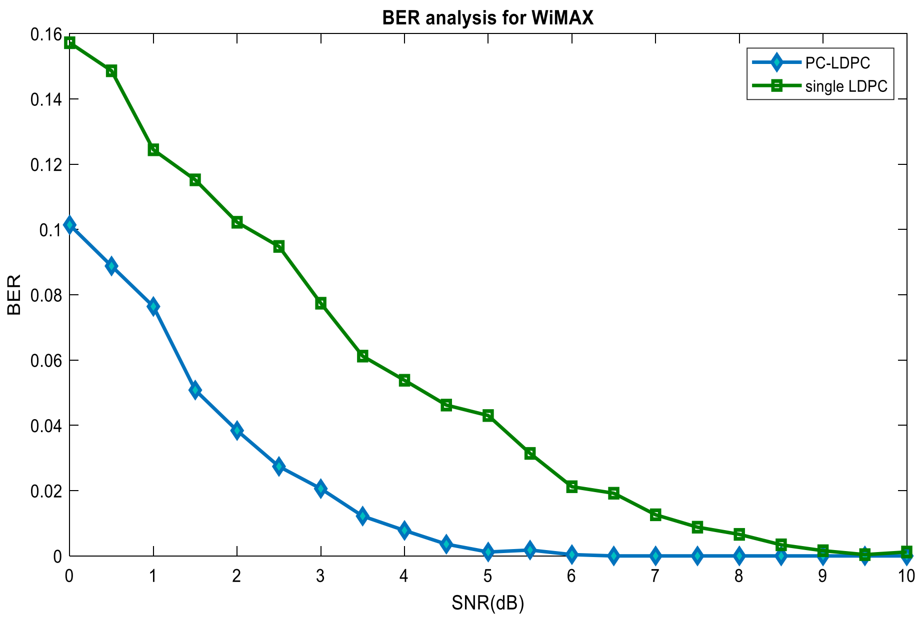

Fig. 32 BER analysis of PC-LDPC codes of OFDM/GFDM system under AWGN channel for WiMAX based simulation using RT Math script module LabVIEW programming

7 Conclusions

GFDM waveform is one of the waveforms as a candidate for 5G. the spectral characteristics of waveform depend on pulse shaping filters. The latency of the system depends on the power spectral density characteristics of the signal. The BER performance of the fifth-generation system depends on the channel coding schemes; the BER computation is required for SNR values in the communication system. In this article, the different prototype filters such as RC, RRC, Gaussian and Xia 4th order filters are applied to the GFDM system under the AWGN channel. The RRC provides out of band power as −37 dB, and Xia's filter generates out of band power as −40 dB, the improvement of 7 dB OOB is observed in RRC, Xia prototype filters corresponding to RC filter. The improvement of 20 dB is observed in GFDM corresponding to the 4G-OFDM signal. Hence, GFDM has less latency than OFDM, is suitable for industry 4.0 and latency applications, and is suitable for 5G candidate waveform. The coding gain of 6.5 dB was observed in the RRC prototype filter based GFDM system under Rayleigh fading channel in PC-LDPC codes corresponding to LDPC codes here BER = 10^{-4} were 12 dB was observed respectively. PC-LDPC-GFDM system in the combination of Xia prototype filter with roll-off factor value 0.5 outperforms other PC-LDPC-GFDM of RC, RRC, Gaussian filters with a coding gain of 3 dB maximum iterations kept as 100. The BER = 10^{-5} for SNR = 9 dB is observed for the Xia filter, with Maximum iterations kept as 200. Hence the coding gain of 12 dB was observed in PC-LDPC codes with Xia 4th order filter corresponding to other prototype filters. PC-LDPC code outperforms the LDPC code up to about 2 dB in the WiMAX scenario with OFDM Transceiver.

Acknowledgements The authors thank the Institute of Aeronautical Engineering for establishing LabVIEW remote laboratory on the campus for making this implementation possible.

Funding The author(s) received no financial support for the research, authorship, and/or publication of this article.

Data Availability The data availability is already explained in this article in the results and discussion section.

Code Availability The authors are ready to share the custom code used to generate the output for the system if needed.

Declarations

Conflict of interest The authors declare that they have no conflict of interest.

References

1. Michailow, N., Matthé, M., Gaspar, I. S., Caldevilla, A. N., Mendes, L. L., Festag, A., & Fettweis, G. (2014). Generalized frequency division multiplexing for 5th generation cellular networks. *IEEE Transactions on Communications, 62*(9), 3045–3061.
2. Michailow, N., Datta, R., Krone, S., Lentmaier, M., & Fettweis, G. (2012, March). Generalized frequency division multiplexing: A flexible multi-carrier modulation scheme for 5th generation cellular networks. In *Proceedings of the German microwave conference (GeMiC'12)* (Vol. 62, pp. 1–4).
3. Michailow, N., Gaspar, I., Krone, S., Lentmaier, M., & Fettweis, G. (2012). Generalized frequency division multiplexing: Analysis of an alternative multi-carrier technique for next generation cellular systems. In *2012 International Symposium on Wireless Communication Systems (ISWCS)* (pp. 171–175). IEEE.

4. Gaspar, D., Mendes, L., & Pimenta, T. (2017). GFDM BER under synchronization errors. *IEEE Communications Letters, 21*(8), 1743–1746.
5. Chung, S. Y., Forney, G. D., Richardson, T. J., & Urbanke, R. (2001). On the design of low-density parity-check codes within 0.0045 dB of the Shannon limit. *IEEE Communications letters, 5*(2), 58–60.
6. Shannon, C. E. (1948). A mathematical theory of communication. *Bell system technical journal, 27*(3), 379–423.
7. Kudekar, S., Richardson, T. J., & Urbanke, R. L. (2011). Threshold saturation via spatial coupling: Why convolutional LDPC ensembles perform so well over the BEC. *IEEE Transactions on Information Theory, 57*(2), 803–834.
8. Shannon, C. E. (2001). A mathematical theory of communication. *ACM SIGMOBILE mobile computing and communications review, 5*(1), 3–55.
9. Adachi, F., & Ohno, K. (1991). BER performance of QDPSK with postdetection diversity reception in mobile radio channels. *IEEE Transactions on Vehicular Technology, 40*(1), 237–249.
10. Naoues, M., Noguet, D., Alaus, L., & Louët, Y. (2011). A common operator for FFT and FEC decoding. *Microprocessors and Microsystems, 35*(8), 708–715.
11. Zhao, J., Zhao, M., Yang, H., Chen, J., Chen, X., & Wang, J. (2011, April). High performance LDPC decoder on CELL BE for WiMAX system. In *2011 Third International Conference on Communications and Mobile Computing* (pp. 278–281). IEEE.
12. Gagan, H. M. R. K. N., Manas, R., & Kumar, N. G. (2017). Performance evaluation of OFDM coding system using concatenated BCH and LDPC codes. *International Journal of Communications, Network and System Sciences, 10*(5), 67–77.
13. Na, Z., Pan, Z., Xiong, M., Liu, X., Lu, W., Wang, Y., & Fan, L. (2018). Turbo receiver channel estimation for GFDM-based cognitive radio networks. *IEEE Access, 6*, 9926–9935.
14. Mostari, L., & Taleb-Ahmed, A. (2018). High performance short-block binary regular LDPC codes. *Alexandria engineering journal, 57*(4), 2633–2639.
15. Matthé, M., Michailow, N., Gaspar, I., & Fettweis, G. (2014). Influence of pulse shaping on bit error rate performance and out of band radiation of generalized frequency division multiplexing. In *2014 IEEE International Conference on Communications Workshops (ICC)* (pp. 43–48). IEEE.
16. Mishra, M., Aich, S., Kim, H. C., & Pradhan, P. M. (2018). A novel ramp-based pulse shaping filter for reducing out of band emission in 5g GFDM system. In *TENCON 2018–2018 IEEE Region 10 Conference* (pp. 0096–0101). IEEE.
17. Kalsotra, S., Kumar, A., Joshi, H. D., Singh, A. K., Dev, K., & Magarini, M. (2019). Impact of Pulse Shaping Design on OOB Emission and Error Probability of GFDM. In *2019 IEEE 2nd 5G World Forum (5GWF)* (pp. 226–231). IEEE.
18. Nagarjuna, T., S. Lakshmi, and K. Nehru. "USRP 2901-based SISO-GFDM transceiver design experiment in virtual and remote laboratory." *The International Journal of Electrical Engineering & Education* (2019): 0020720919857620.
19. Mhaske, S., Uliana, D., Kee, H., Ly, T., Aziz, A., & Spasojevic, P. (2015). A 2.48 Gb/s QC-LDPC Decoder Implementation on the NI USRP-2953R. *arXiv preprint* arXiv:1505.04339.
20. Chitnis, N., Joshi, T., Padte, S., Donde, S., & Karia, D. (2018). Hard decoding based design of regular LDPC using LabVIEW. In *2018 International Conference on Current Trends towards Converging Technologies (ICCTCT)* (pp. 1–4). IEEE.
21. Barakatain, M., & Kschischang, F. R. (2018). Low-complexity concatenated LDPC-staircase codes. *Journal of Lightwave Technology, 36*(12), 2443–2449.
22. Aswathy, G. P., & Haneefa, N. K. (2016). A Survey on Methods of Parallel Concatenation of LDPC Codes. *International Journal of Engineering and Advanced Technology, 5*(4), 124–129.
23. Merah, H., Mesri, M., & Tahkoubit, K. (2018). Significant reduction of bit error rate in 5G-Gfdm system using concatenated turbo code with low density parity check code in fading channels. *Journal of Electrical Systems, 14*(1), 118–129.
24. Hu, X. Y., Eleftheriou, E., Arnold, D. M., & Dholakia, A. (2001). Efficient implementations of the sum-product algorithm for decoding LDPC codes. In *GLOBECOM'01. IEEE Global Telecommunications Conference (Cat. No. 01CH37270)* (Vol. 2, pp. 1036–1036E). IEEE.
25. National Instruments, USRP-2901 Block Diagram, http://www.ni.com/documentation/en/usrpsoftware-defined-radio-device/latest/usrp2901/block-diagram/

Publisher's Note Springer Nature remains neutral with regard to jurisdictional claims in published maps and institutional affiliations.

Nagarjuna Telagam is with the Electronics and Communication Engineering Department, GITAM, Bangalore, India. He is a Research Scholar in Sathyabama University and is interested in the following topics: Wireless Communications, MIMO, OFDM, GFDM. Currently, He Received his B.Tech degree from JNTU University/ Narayana Engineering College. He received his master degree from Anna University/ Loyola Institute of Technology. He is Anna University rank holder(20) for M.E degree in 2013. He published papers in different Scopus Indexed Journals

S. Lakshmi is Professor in the Department of Electronics and Communication Engineering. She finished her phD in the area of wirless networks, she completed masters degree in applied electronics, she handled many UG courses and has more than 15 years of experience in teaching and research. She can be reached at lakshmi.ece@sathyabama.ac.in. Her area of interest includes MIMO, Wireless networks

Nehru Kandasamy received his Bachelor Degree in Erode Sengunthar Engineering College, Anna University in 2005. And he obtained his Master Degree in R.M.K Engineering, Anna University in 2007.And he also obtained outstanding master student at that year. He is obtained his Ph.D in 2014 at Faculty of Information and Communication Engineering, Anna University, India. His main research interest is in the area of Low Power VLSI, Testing of VLSI Circuits, FPGA Design, CAD for VLSI, Signal processing